Electronic Supplementary Material (ESI) for RSC Advances.

Electronic Supporting Informations

Solvatochromic studies of pull-push molecules containing dimethylaniline and aromatic hydrocarbon linked by acetylene unit

Irena Bylińska, Małgorzata Wierzbicka, Cezary Czaplewski, Wiesław Wiczk*

Faculty of Chemistry, University of Gdańsk

80-308 Gdańsk, Wita Stwosza 63, Poland

Table 1 ESI Solvent properties (n-refractive index, ε- electric permittivity and Kamlet-Taft (α,β,π^*) and Catalan (SP, SdP, SB,SA) empirical solvent parameters.

	Solvent	n[1,2]	ε[2,3]	E_T^N [1,2,4]	α [2,3,5]	β	π*	SP[6]	SdP	SB	SA
1	MeOH	1.3306	32.63	0.762	0.98	0.66	0.6	0.86	0.9	0.55	0.61
2	EtOH	1.3594	24.55	0.654	0.86	0.75	0.54	0.85	0.78	0.66	0.4
3	*iso*-propyl alcohol (iPrOH)	1.38126	18.3	0.546	0.76	0.84	0.48	0.85	0.81	0.83	0.28
4	2,2,2-trifluoroethanol (TFE)	1.291	26.67	0.898	1.51	0	0.73	0.91	0.92	0.11	0.89
5	hexafluoro-2-propanol (HFiP)	1.277	16.62	1.07	1.96	0	0.65	1.014	--	0.014	1.01
6	n-hexane	1.3726	1.89	0.01	0	0	-0.011	0.519	0	0.056	0
7	*iso*-octane	1.3914	1.843	0.01	0	0	0.01	0.54	0	0.08	0
8	n-hexadecane	1.4345	2.05	0.009	0	0	0.03	0.578	0	0.086	0
9	squalane (SQ)	1.453	2.23	--	--	--	--	--	0	0.05	0
10	cyclohexane	1.4263	2.023	0.006	0	0	0	0.56	0	0.07	0
11	toluene	1.49718	2.38	0.099	0	0.11	0.54	0.68	0.28	0.13	0
12	1-chloro-n-propane	1.388	8.59	0.207	--	--	--	--	--	--	--
13	1-chloro-n-butane	1.4	7.39	0.19	0	0	0.39	0.84	0.529	0.138	0
14	1-chloro-n-hexane	1.419	6.1	--	--	--	--	--	--	--	--
15	1-chloro-n-octane	1.43	5.1	--	--	--	--	--	--	--	--
16	1-chloro-n-decane	1.438	4.58	--	--	--	--	--	--	--	--
17	1-chloro-n-hexadecane	1.45	3.7	--	--	--	--	--	--	--	--
18	acetone	1.3588	20.7	0.355	0.08	0.48	0.62	0.881	0.91	0.475	0
19	acetonitrile	1.34596	37.5	0.46	0.19	0.4	0.66	0.895	0.97	0.286	0.044
20	1,4-dioxane	1.422	2.235	0.164	0	0.37	0.55	0.7	0.31	0.44	0
21	tetrahydrofuran (THF)	1.407	7.6	0.207	0	0.55	0.58	0.84	0.63	0.59	0
22	2-methyl-tetrahydrofuran (MeTHF)	1.4051	5.26	0.179	0	0.45	0.48	0.717	0.77	0.584	0
23	Diethyl eter (Et_2O)	1.3526	4.2	0.117	0	0.47	0.24	0.694	0.39	0.562	0
24	Ethyl acetate (AcOEt)	1.3726	6.11	0.228	0	0.45	0.55	0.8	0.6	0.54	0
25	N,N-dimethylformamide (DMF)	1.431	37	0.386	0	0.69	0.88	0.954	0.98	0.613	0.031
26	Dimethyl sulfoxide (DMSO)	1.479	46.7	0.444	0	0.76	1	1	1	0.647	0.072

[1] P.J. Cerón-Carrascoa, D. Jacquemin, C. Laurence, A. Planchat, C. Reichardt, K. Sraïdi, J. Phys. Org. Chem., 2014, **27**, 512

[2] E. Krystkowiak, A. Maciejewski, Phys. Chem. Chem. Phys., 2011, **13,** 11317

[3]Z. Pawlowska, A. Lietard, S. Aloïse, M. Sliwa, A. Idrissi, O. Poizat, G. Buntinx, S. Delbaere, A. Perrier, F. Maurel, P. Jacques, J. Abe, Phys. Chem. Chem. Phys., 2011, **13**, 13185

[4] C. Reichardt, Chem. Rev., 1994, **94**, 2319

[5] A. de Juan, G. Fonrodona, E. Casassas, Trends in analytical chemistry, 1997, **16**, 52

[6] J. Catalàn, J. Phys. Chem. B., 2009, **113**, 5951

Table 2 ESI. Half-width of emission spectra of 1NacDMA and 2NacDMA in protic solvents.

hw [cm^{-1}]		
solvent	1NacDMA	2NacDMA
HFiP	4800	5700
TFE	5300	6400
MeOH	4900	4950
EtOH	4450	4700
iPrOH	4450	4700

Table 3 ESI Intercept, slope and coefficient of the quality of fit (r^2) estimated from the dependence of a given photophysical parameter on solvent polarity index E^N_T for compounds studied. N.p. denote number of solvents used for a linear correlation.

quantity	intercept	slope	r^2	N.p.
1NacDMA				
ν_{abs}^{max} [cm^{-1}]	28838±96	-2584±398	0.7509	16
ν_{fluo}^{max} [cm^{-1}]	26370±229 24716±418	-15208±934 -4921±63	0.9489 0.9837	16 3(protic)
$\Delta\nu = \nu_{abs}^{max} - \nu_{fluo}^{max}$ [cm^{-1}]	2468±187 4002±384	12624±771 4699±528	0.9748 0.9755	16 4 (protic)
ϕ	0.91±0.05	-1.05±0.2	0.6581	16
τ [ns]	0.93±1.62	-5.02±0.6	0.8002	16
$k_f * 10^{-8}$ [s^{-1}]	7.28±0.37	-14.4±1.5	0.8617	16
$k_{nr} * 10^{-8}$ [s^{-1}]	1.03±0.38	2.55±1.59	0.1560	16
$\mu * 10^5$ [cm^3/s]	2.05±0.06	-2.62±0.23	0.9062	15
2NacDMA				
ν_{abs}^{max} [cm^{-1}]	27206±66	435±192	0.2309	19
ν_{fluo}^{max} [cm^{-1}]	27050±237 25710±665	-16124±979 -5227±1008	0.9509 0.9642	16 3 (protic)
$\Delta\nu = \nu_{abs}^{max} - \nu_{fluo}^{max}$ [cm^{-1}]	1161±276 1158±1045	16512±1137 7862±1438	0.9378 0.9442	16 4 (protic)
ϕ	0.870±0.048	-0.708±0.199	0.4749	16
τ [ns]	0.74±0.17	5.08±0.71	0.7861	16
$k_f * 10^{-8}$ [s^{-1}]	8.11±0.37	-14.9±1.5	0.8724	16
$k_{nr} * 10^{-8}$ [s^{-1}]	1.48±0.37	0.73±1.52	0.0163	16
$\mu * 10^5$ [cm^3/s]	2.69±0.16	-3.79±0.56	0.8224	12
AacDMA				
ν_{abs}^{max} [cm^{-1}]	22783±57	257±165	0.1254	17
ν_{fluo}^{max} [cm^{-1}]	21993±181 20657±373	-12778±747 -3829±513	0.9544 0.9653	16 4 (protic)
$\Delta\nu = \nu_{abs}^{max} - \nu_{fluo}^{max}$ [cm^{-1}]	854±181 924±637	12588±747 6182±876	0.9530 0.9614	16 4 (protic)
ϕ	0.76±0.06 1.43±0.07	-0.76±0.23 -1.63±0.10	0.4354 0.9899	16 4 (protic)
τ [ns]	3.09±0.18 8.90±0.03	2.77±0.76 -9.00±0.04	0.4857 0.9999	16 3 (protic)
$k_f * 10^{-8}$ [s^{-1}]	2.41±0.08 2.95±0.02	-3.42±0.35 -2.65±0.03	0.8736 0.9998	16 3 (protic)
$k_{nr} * 10^{-8}$ [s^{-1}]	8.97±1.91	9.98±7.91	0.1021	16
$\mu * 10^5$ [cm^3/s]	1.00±0.04 1.19±0.03	-1.43±0.15 -0.99±0.04	0.8601 0.9984	16 3 (protic)

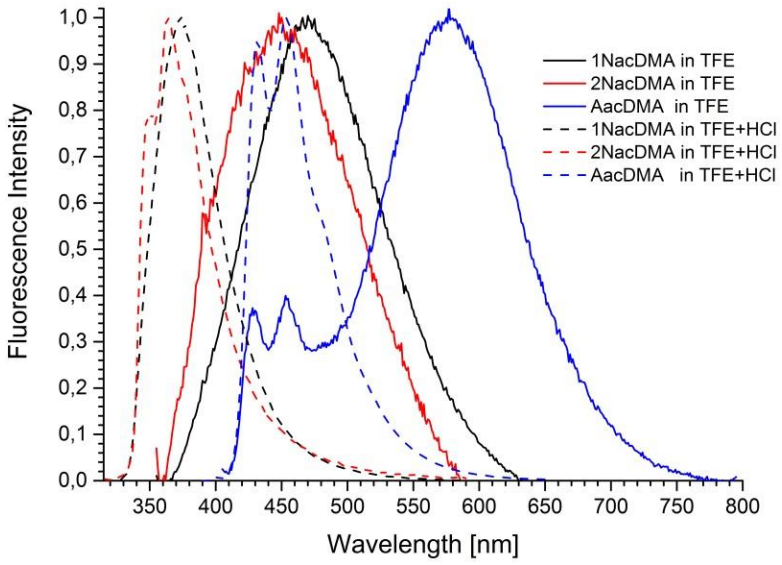

Fig. 1 ESI Fluorescence spectra of 1NacDMA, 2NacDMA and AacDMA measured in TFE and acidified TFE (3 ml TFE+1 µl concentrated HCl)

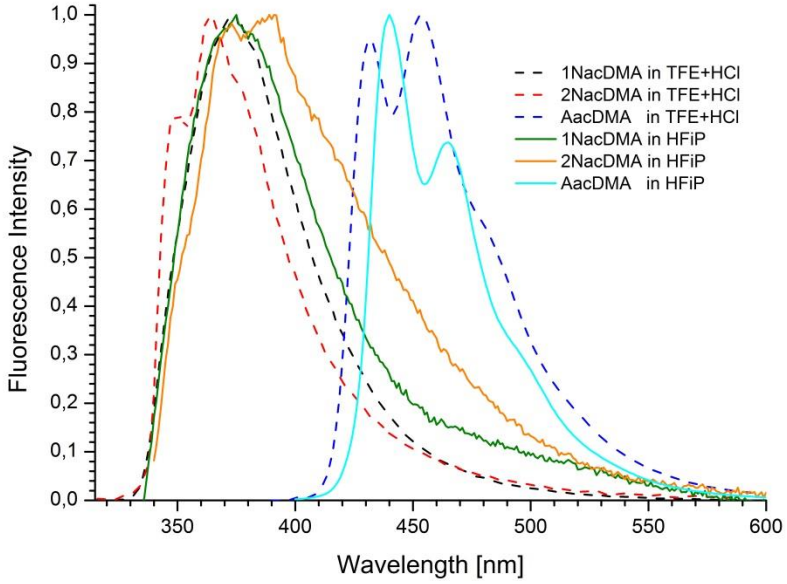

Fig. 2 ESI Fluorescence spectra of 1NacDMA, 2NacDMA and AacDMA measured in acidified TFE (3 ml TFE+1 µl concentrated HCl) and HFiP.

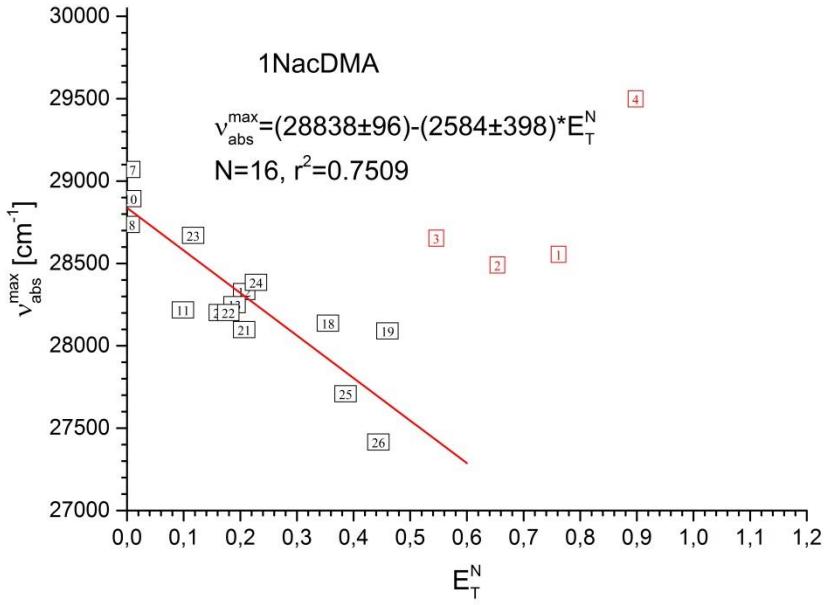

Fig. 3 ESI Plot of the correlation of ν_{abs}^{max} *versus* E_T^N for 1NacDMA. The red points were not taken into account in the correlation. Numbers in the squares correspond to the order of the solvents in Tables 1-3 in the main text of publication.

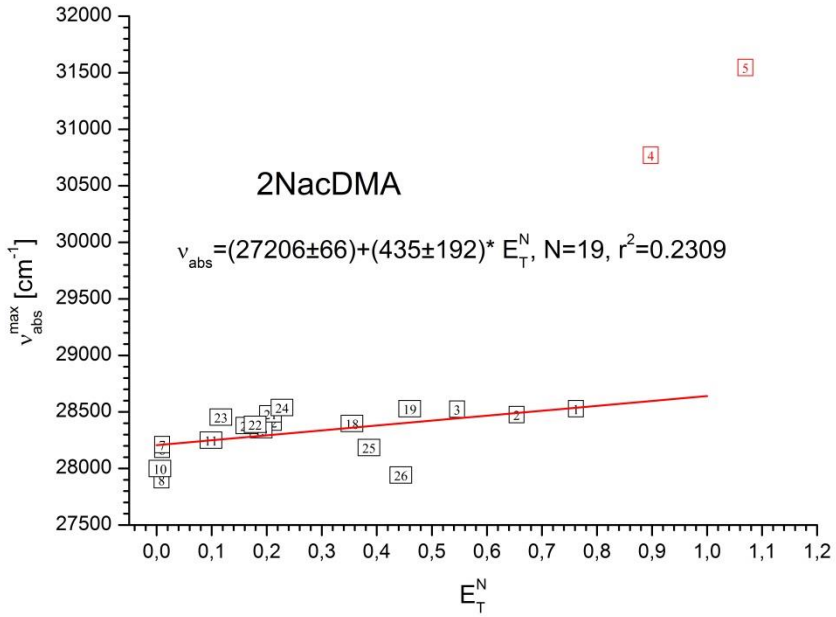

Fig. 4 ESI Plot of the correlation of ν_{abs}^{max} *versus* E_T^N for 2NacDMA. The red points were not taken into account in the correlation. Numbers in the squares correspond to the order of the solvents in Tables 1-3 in the main text of publication.

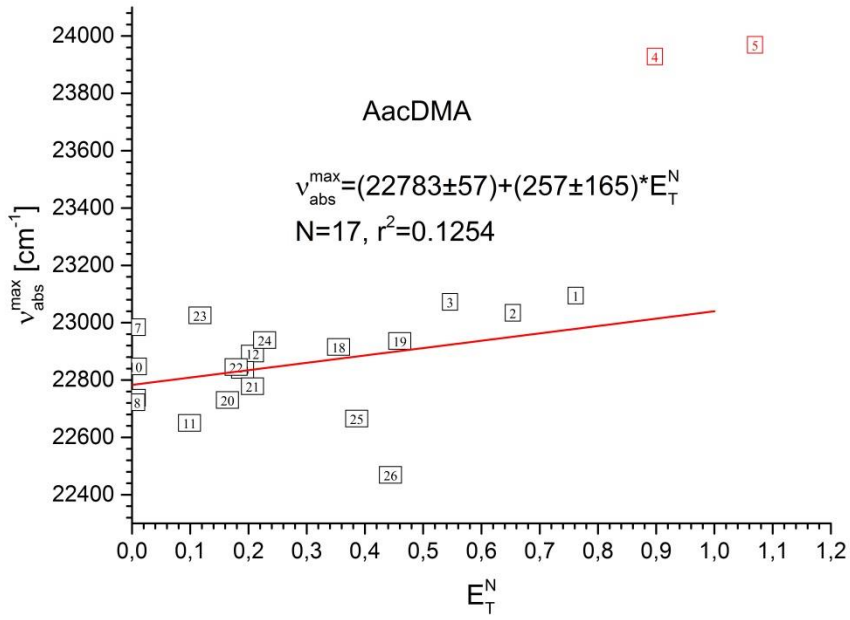

Fig. 5 ESI Fig. 4 ESI Plot of the correlation of ν_{abs}^{max} *versus* E_T^N for AacDMA. The red points were not taken into account in the correlation. Numbers in the squares correspond to the order of the solvents in Tables 1-3 in the main text of publication.

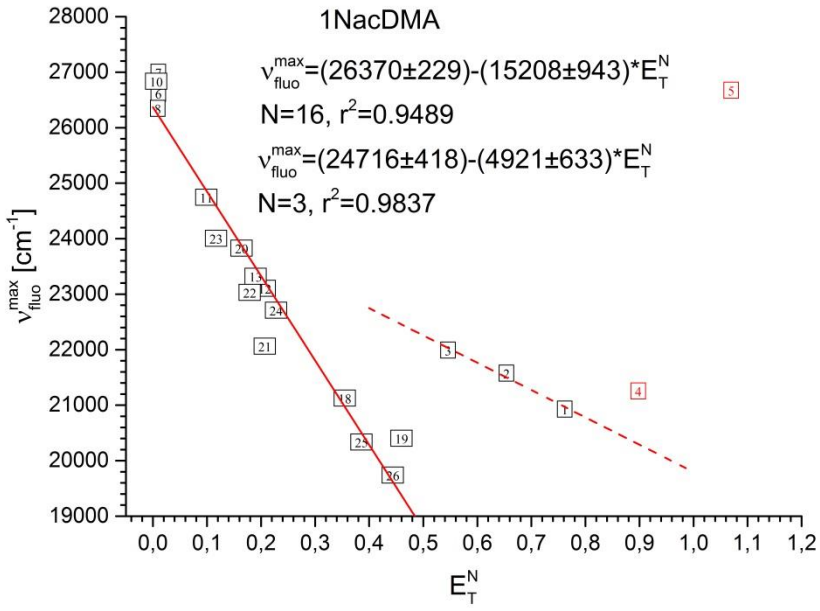

Fig. 6 ESI Plot of the correlation of ν_{fluo}^{max} *versus* E_T^N for 1NacDMA. Solid line for aprotic solvents, dashed line for protic solvents. The red points were not taken into account in the correlation. Numbers in the squares correspond to the order of the solvents in Tables 1-3 in the main text of publication.

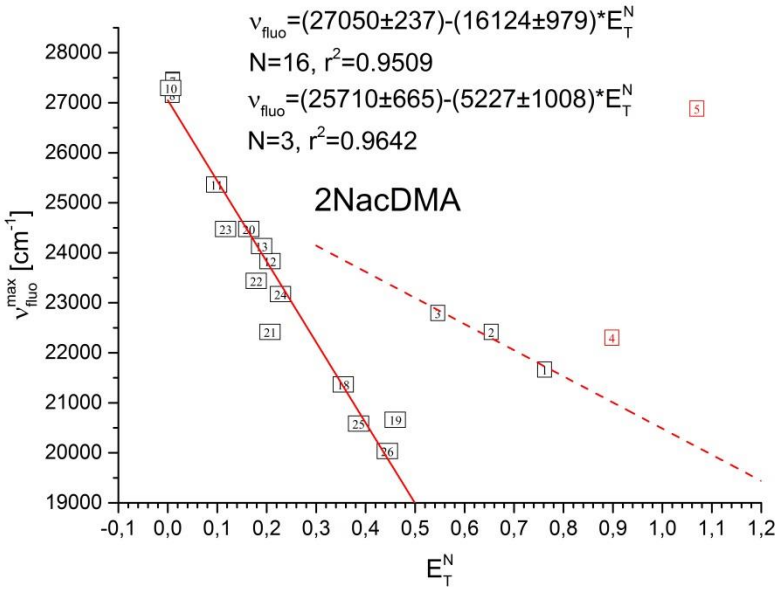

Fig. 7 ESI Plot of the correlation of ν_{fluo}^{max} *versus* E_T^N for 2NacDMA. Solid line for aprotic solvents, dashed line for protic solvents. The red points were not taken into account in the correlation. Numbers in the squares correspond to the order of the solvents in Tables 1-3 in the main text of publication.

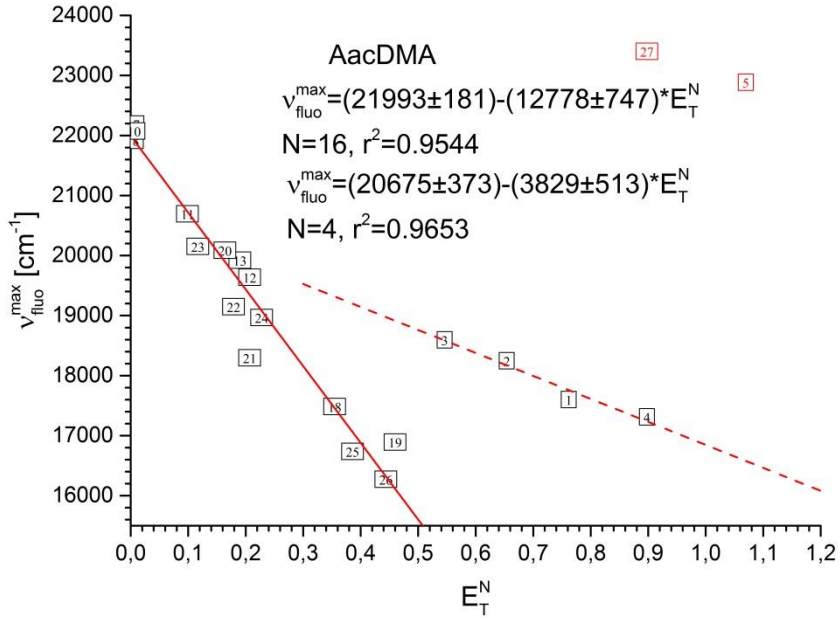

Fig. 8 ESI Plot of the correlation of ν_{fluo}^{max} *versus* E_T^N for AacDMA. Solid line for aprotic solvents, dashed line for protic solvents. The red points were not taken into account in the correlation. Numbers in the squares correspond to the order of the solvents in Tables 1-3 in the main text of publication.

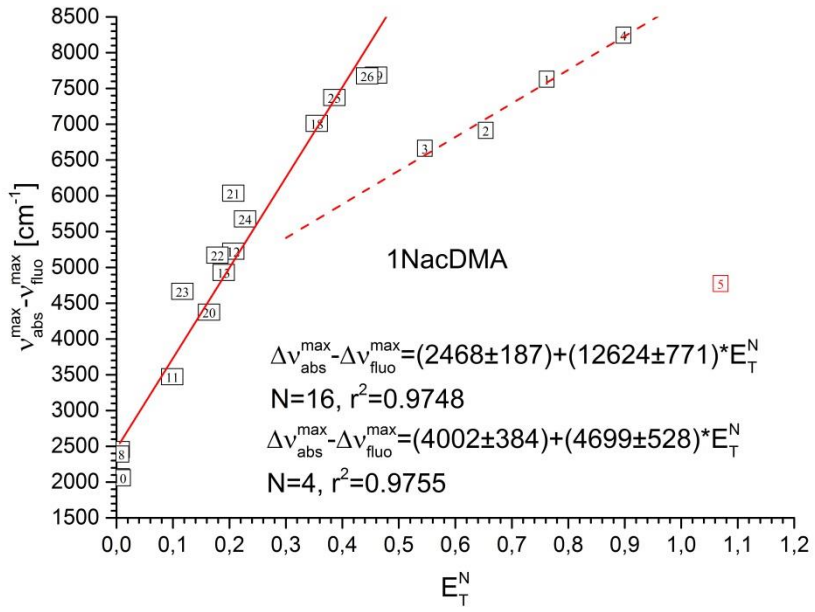

Fig. 9 ESI Plot of the correlation of $\nu_{abs}^{max} - \nu_{fluo}^{max}$ *versus* E_T^N for 1NacDMA. Solid line for aprotic solvents, dashed line for protic solvents. The red points were not taken into account in the correlation. Numbers in the squares correspond to the order of the solvents in Tables 1-3 in the main text of publication.

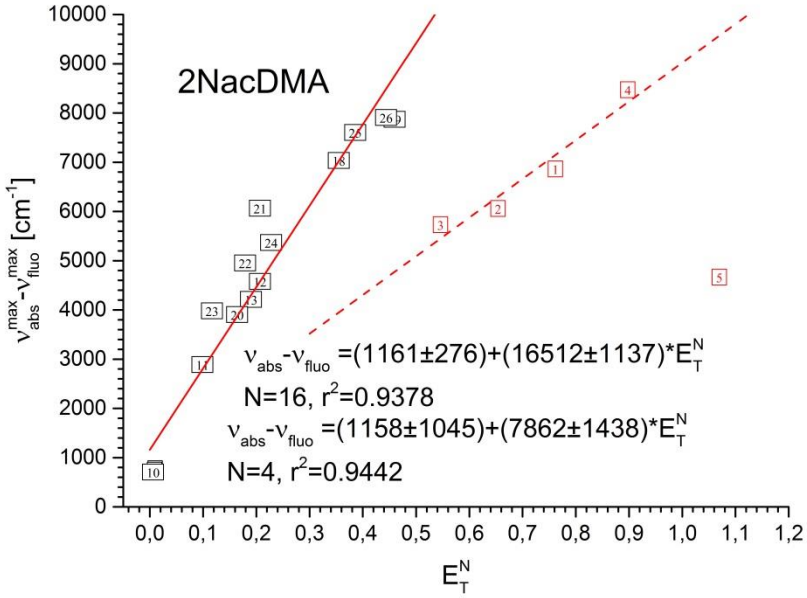

Fig. 10 ESI Plot of the correlation of $\nu_{abs}^{max} - \nu_{fluo}^{max}$ *versus* E_T^N for 2NacDMA. Solid line for aprotic solvents, dashed line for protic solvents. The red points were not taken into account in the correlation. Numbers in the squares correspond to the order of the solvents in Tables 1-3 in the main text of publication.

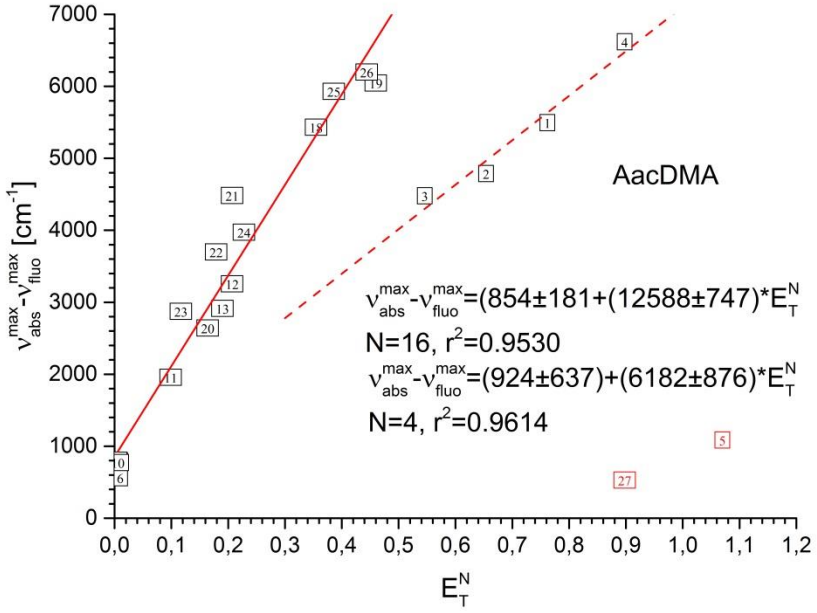

Fig. 11 ESI Plot of the correlation of $\nu_{abs}^{max} - \nu_{fluo}^{max}$ *versus* E_T^N for AacDMA. Solid line for aprotic solvents, dashed line for protic solvents. The red points were not taken into account in the correlation. Numbers in the squares correspond to the order of the solvents in Tables 1-3 in the main text of publication.

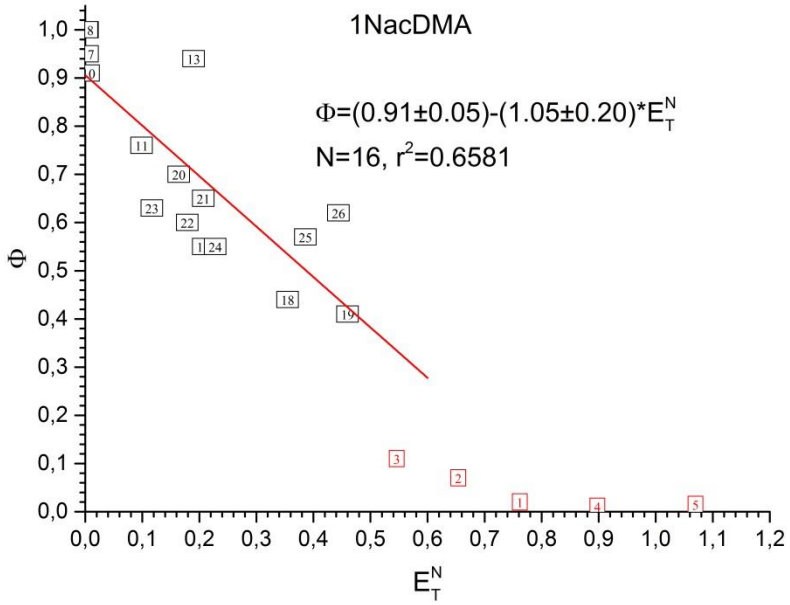

Fig. 12 ESI Plot of the correlation of fluorescence quantum yields (Φ) *versus* E_T^N for 1NacDMA.. The red points were not taken into account in the correlation. Numbers in the squares correspond to the order of the solvents in Tables 1-3 in the main text of publication.

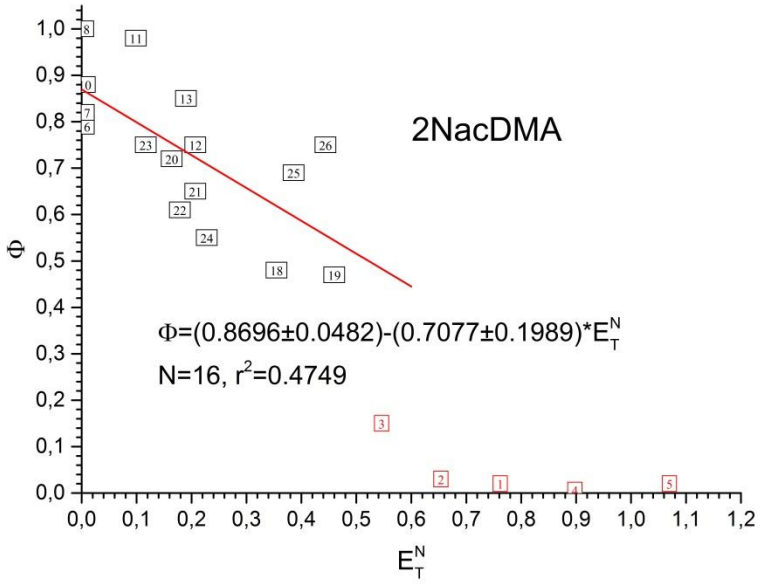

Fig. 13 ESI Plot of the correlation of fluorescence quantum yields (Φ) *versus* E_T^N for 2NacDMA. The red points were not taken into account in the correlation. Numbers in the squares correspond to the order of the solvents in Tables 1-3 in the main text of publication.

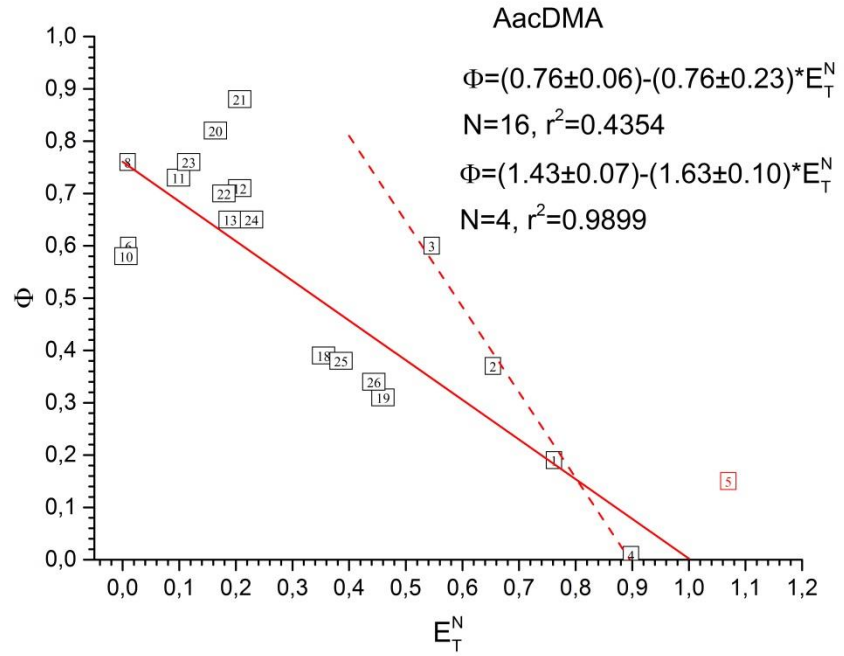

Fig. 14 ESI Plot of the correlation of fluorescence quantum yields (Φ) *versus* E_T^N for AacDMA. Solid line for aprotic solvents, dashed line for protic solvents. The red points were not taken into account in the correlation. Numbers in the squares correspond to the order of the solvents in Tables 1-3 in the main text of publication.

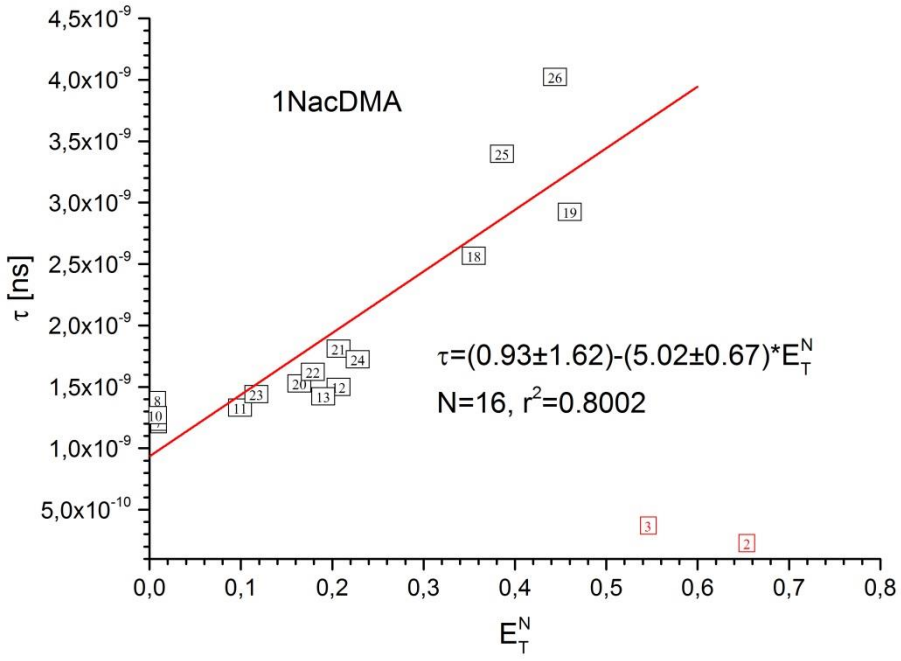

Fig. 15 ESI Plot of the correlation of fluorescence lifetimes (τ) v*ersus* E_T^N for 1NacDMA. The red points were not taken into account in the correlation. Numbers in the squares correspond to the order of the solvents in Tables 1-3 in the main text of publication.

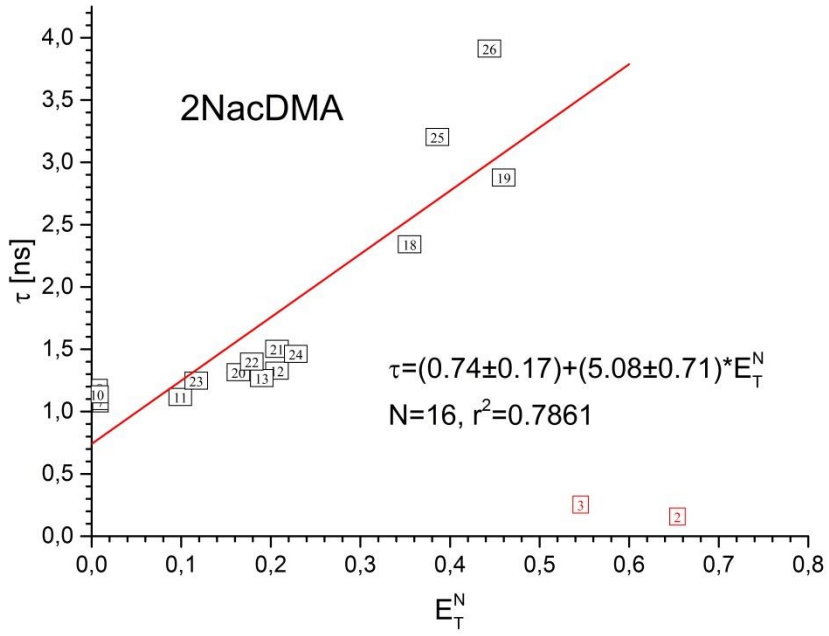

Fig. 16 ESI Plot of the correlation of fluorescence lifetimes (τ) v*ersus* E_T^N for 2NacDMA. The red points were not taken into account in the correlation. Numbers in the squares correspond to the order of the solvents in Tables 1-3 in the main text of publication.

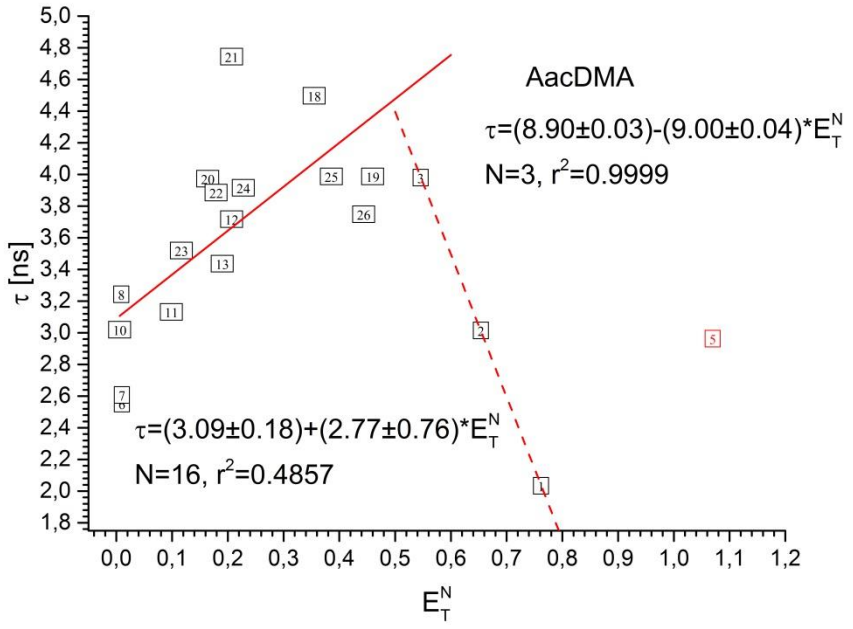

Fig. 17 ESI Plot of the correlation of fluorescence lifetimes (τ) v*ersus* E_T^N for AacDMA. Solid line for aprotic solvents, dashed line for protic solvents. The red points were not taken into account in the correlation. Numbers in the squares correspond to the order of the solvents in Tables 1-3 in the main text of publication.

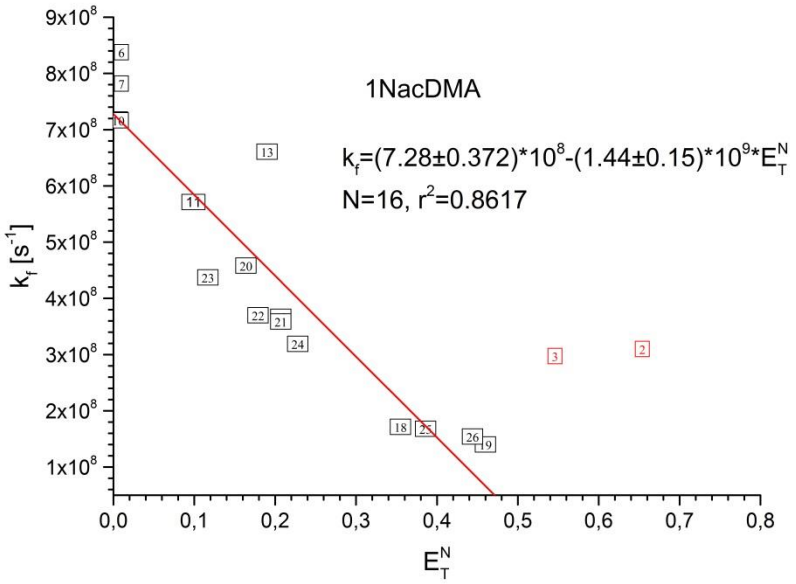

Fig. 18 ESI Plot of the correlation of fluorescence rate constants (k_f) v*ersus* E_T^N for 1NacDMA. The red points were not taken into account in the correlation. Numbers in the squares correspond to the order of the solvents in Tables 1-3 in the main text of publication.

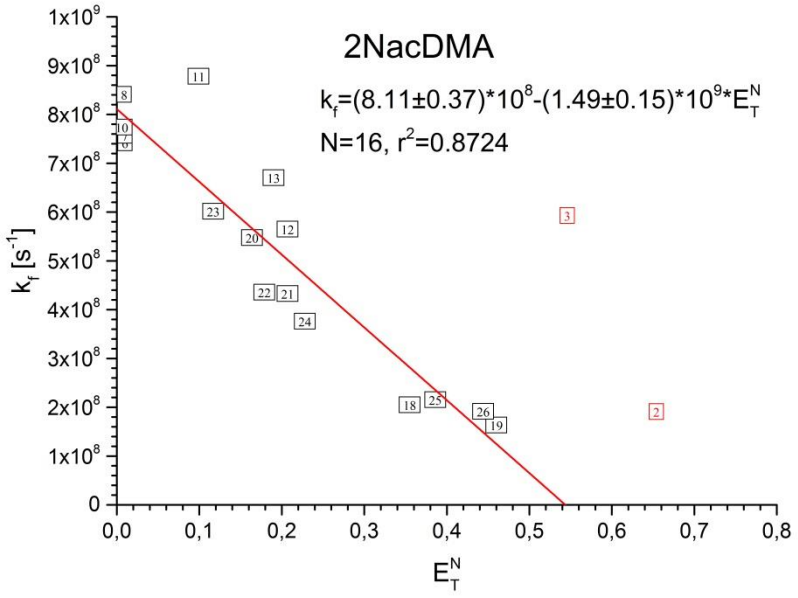

Fig. 19 ESI Plot of the correlation of fluorescence rate constants (k_f) *versus* E_T^N for 2NacDMA. The red points were not taken into account in the correlation. Numbers in the squares correspond to the order of the solvents in Tables 1-3 in the main text of publication.

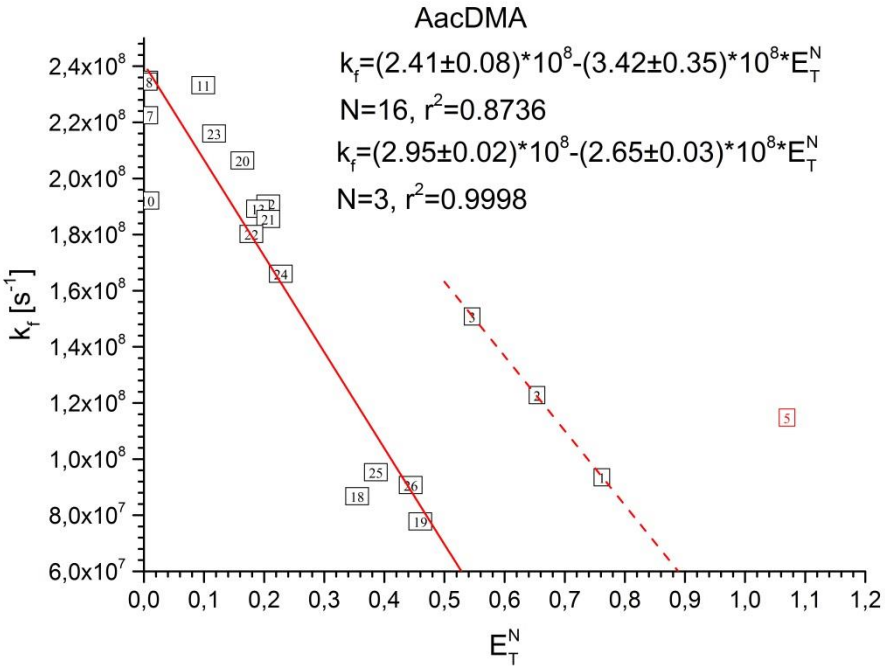

Fig. 20 ESI Plot of the correlation of fluorescence rate constants (k_f) *versus* E_T^N for AacDMA. Solid line for aprotic solvents, dashed line for protic solvents. The red points were not taken into account in the correlation. Numbers in the squares correspond to the order of the solvents in Tables 1-3 in the main text of publication.

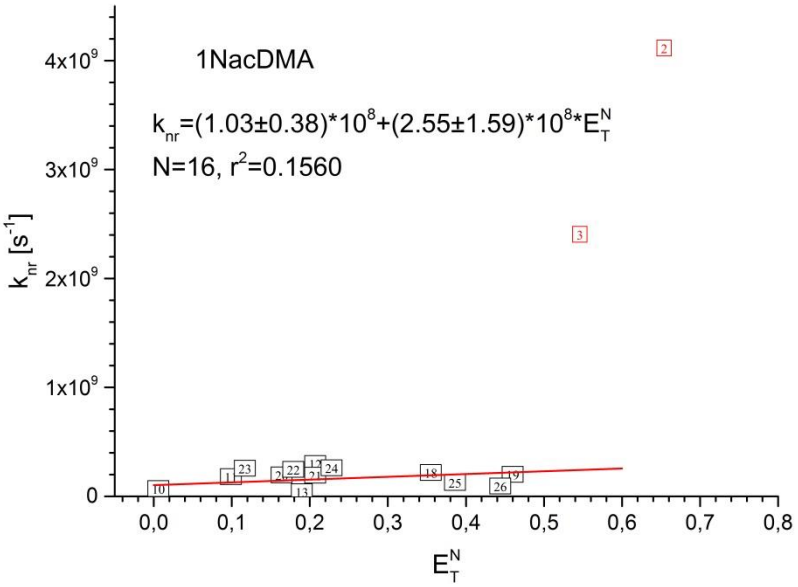

Fig. 21 ESI Plot of the correlation of non-radiative rate constants (k_{nr}) *versus* E_T^N for 1NacDMA. The red points were not taken into account in the correlation. Numbers in the squares correspond to the order of the solvents in Tables 1-3 in the main text of publication.

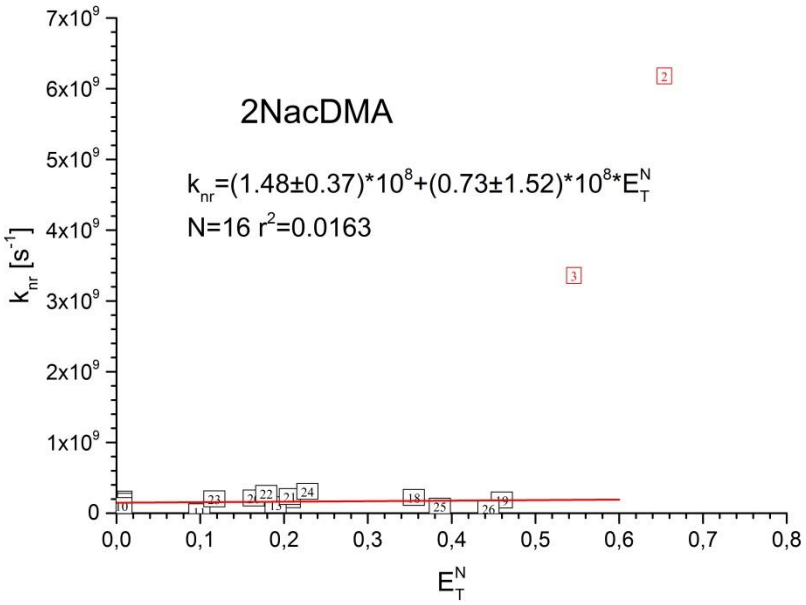

Fig. 22 ESI Plot of the correlation of non-radiative rate constants (k_{nr}) *versus* E_T^N for 2NacDMA. The red points were not taken into account in the correlation. Numbers in the squares correspond to the order of the solvents in Tables 1-3 in the main text of publication.

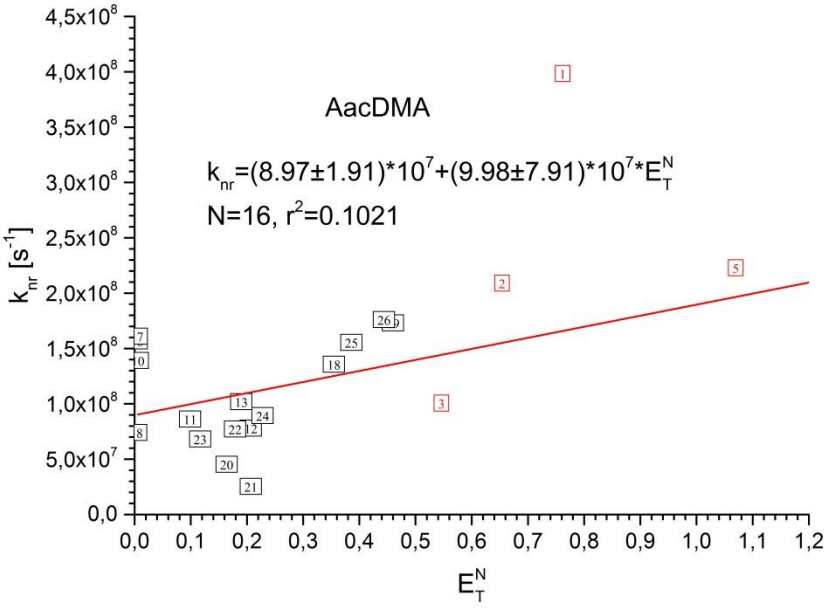

Fig. 23 ESI Plot of the correlation non-radiative rate constants (k_{nr}) v*ersus* E_T^N for AacDMA. Solid line for aprotic solvents, dashed line for protic solvents. The red points were not taken into account in the correlation. Numbers in the squares correspond to the order of the solvents in Tables 1-3 in the main text of publication.

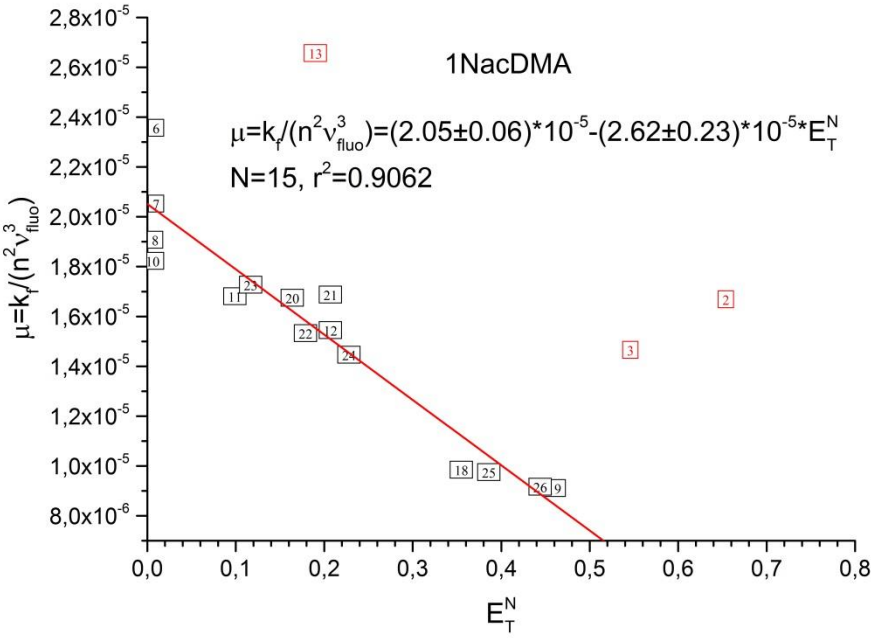

Fig. 24 ESI Plot of the correlation of transition dipole moments (μ) v*ersus* E_T^N for 1NacDMA. The red points were not taken into account in the correlation. Numbers in the squares correspond to the order of the solvents in Tables 1-3 in the main text of publication.

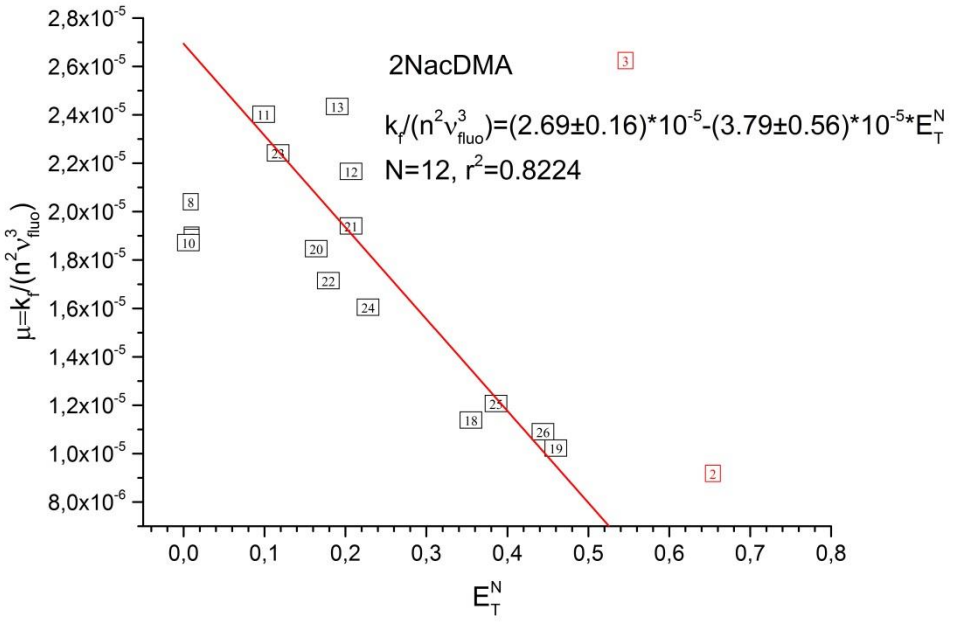

Fig. 25 ESI Plot of the correlation of transition dipole moments (μ) v*ersus* E_T^N for 2NacDMA. The red points were not taken into account in the correlation. Numbers in the squares correspond to the order of the solvents in Tables 1-3 in the main text of publication.

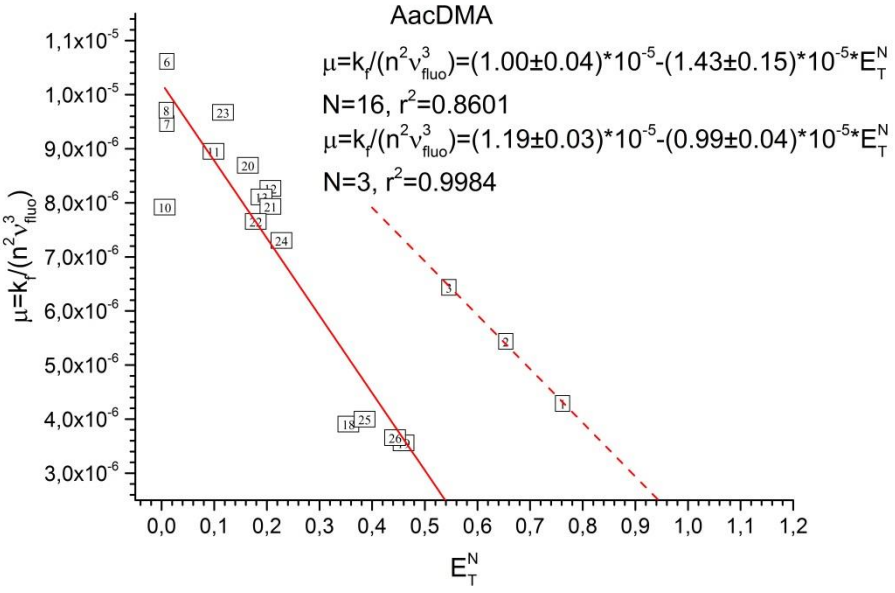

Fig. 26 ESI Plot of the correlation of transition dipole moments (μ) v*ersus* E_T^N for AacDMA. Solid line for aprotic solvents, dashed line for protic solvents.The red points were not taken into account in the correlation. Numbers in the squares correspond to the order of the solvents in Tables 1-3 in the main text of publication.

Table 4 ESI Estimated from eqn (5) adjusted coefficients $(v_x)_0$, a_{SP}, b_{SdP}, c_{SB}, d_{SA} their standard error and correlation coefficient (r^2) of the multiple linear correlation analysis of absorption (v_{abs}), fluorescence (v_{fluo}) wavenumber, Stokes shift (Δv_{SS}), fluorescence quantum yield (ϕ), fluorescence (k_f) and nonradiative (k_{nr}) rate constant and value proportional to squared transition dipole moment (μ^2)~$k_f/(n^2\ v_{fluo}^3$) of 1NacDMA as a function of Catalan-four parameter solvent scale. N.p. denote number of solvent using in the analysis.

	$(v_x)_0$	a_{SP}	b_{SdP}	c_{SB}	d_{SA}	r^2	N.p.
v_{abs} [cm^{-1}]	31672±378	-4198±553	-786±123	-135±161	379±175	0.9471	20
	31660±374	-4195±548	-859±86	-	775±168	0.9446	20
v_{fluo} [cm^{-1}]	29613±2226	-4320±3256	-5166±728	1940±947	1755±1029	0.9229	20
Δv_{SS} [cm^{-1}]	2964±1898	122±2276	4380±620	1805±808	-1016±877	0.9242	20
	2145±255	-	4385±589	1805±782	-1040±669	0.9241	20
φ	0.38±0.29	0.90±0.42	-0.26±0.09	-0.47±0.12	-0.68±0.13	0.9350	20
τ [ns]	-2.34±1.57	5.10±2.30	2.17±0.55	-0.94±0.85	-4.26±1.42	0.7761	18
	-2.48±1.58	5.15±2,32	1.73±0.32	-	-4.86±1.33	0.7551	18
k_f*10^8[s^{-1}]	8.24±2.30	-0.65±3.37	-4.93±0.80	-2.26±1.24	2,02±2.07	0.9229	18
	7,72±0.32	-	-5.02±0.76	-1.71±1.11	-	0.9155	18
	7.53±3.04	-	-5.95±0.49	-	-	0.9022	18
$k_{nr}*10^8$[s^{-1}]	11.67±6.80	-15.99±9.94	-2.76±2.37	3.70±3.67	89.90±6.12	0.9655	18
	12.99±6.53	-17.90±9.35	-	-	90.54±5.00	0.9618	18
μ^2*10^5	2.88±1.06	-1.07±1.54	-0.84±0.37	-0.30±0.57	0.63±0.95	0.6099	18
[cm^3/s]	2.12±0.13	-	-0.96±0.21	-	-	0.5685	18

Table 5 ESI Estimated from eqn (5) adjusted coefficients $(v_x)_0$, a_{SP}, b_{SdP}, c_{SB}, d_{SA} their standard error and correlation coefficient (r^2) of the multiple linear correlation analysis of absorption (v_{abs}), fluorescence (v_{fluo}) wavenumber, Stokes shift (Δv_{SS}), fluorescence quantum yield (ϕ), fluorescence (k_f) and nonradiative (k_{nr}) rate constant and value proportional to squared transition dipole moment (μ^2)~$k_f/(n^2\ v_{fluo}^3)$ of 2NacDMA as a function of Catalan-four parameter solvent scale. N.p. denote number of solvent using in the analysis.

	$(v_x)_0$	a_{SP}	b_{SdP}	c_{SB}	d_{SA}	r^2	N.p.
v_{abs} [cm^{-1}]	299099±1065	-2474±155	636±348	-766±453	1148±492	0.7214	20
v_{fluo} [cm^{-1}]	29588±1531	-3646±2214	-64941±495	327±644	-277±699	0.9682	20
	29129±1136	-2900±1637	-6412±287	-	-	0.9671	20
Δv_{SS} [cm^{-1}]	320±2063	1171±3018	7130±675	-1094±878	1426±954	0.9525	20
	11131±279	-	71841±642	-1096±854	1198±730	0.9520	20
Φ	-0.23±0.26	1.73±0.39	-0.19±0.09	-0.42±0.11	-0.63±0.11	0.9428	20
τ [ns]	-2.40±1.67	4.95±2.44	2.29±0.58	-1.17±0.90	-3.81±1.50	0.7497	18
	-2.57±1.70	5.00±2.50	1.73±0.40	-	-4.53±1.43	0.7171	18
k_f*10^8[s^{-1}]	4.84±3.94	5.29±5.75	-6.45±1.37	-2.03±2.12	1,07±3.54	0.8170	18
	8.42±4.76	-	-6.23±0.77	-	-	0.8061	18
$k_{nr}*10^9$[s^{-1}]	2.02±1.03	-2.74±1.50	-0.43±0.36	0.32±0.56	13.58±0.93	0.9643	18
	2.07±1.47	-2,75±1,47	-0.28±0.23	-	13.78±0.08	0.9634	18
	2.29±1.00	-3.24±1.34	-	-	13.40±0.08	0.9597	18
μ^2*10^5	1.98±1.44	0.19±2.10	-1.21±0.50	-0.82±0.78	-0.48±1.30	0.3929	18
[cm^3/s]	2.20±0.28	-	-0.81±0.28	-	-	0.3399	18
	0.39±1.09	2.58±1.59	-0.48±0.40	-0.18±0.56	-12.65±5.54	0.6939	16*
	0.43±1.04	2.49±1.51	0.58±0.25	-	-12.15±5.12	0,6909	16

Table 6 ESI Estimated from eqn (5) adjusted coefficients $(v_x)_0$, a_{SP}, b_{SdP}, c_{SB}, d_{SA} their standard error and correlation coefficient (r^2) of the multiple linear correlation analysis of absorption (v_{abs}), fluorescence (v_{fluo}) wavenumber, Stokes shift (Δv_{SS}), fluorescence quantum yield (ϕ), fluorescence (k_f) and nonradiative (k_{nr}) rate constant and value proportional to squared transition dipole moment (μ^2)~$k_f/(n^2\ v_{fluo}{}^3$) of AacDMA as a function of Catalan-four parameter solvent scale. N.p. denote number of solvent using in the analysis.

	$(v_x)_0$	a_{SP}	b_{SdP}	c_{SB}	d_{SA}	r^2	N.p.
v_{abs} [cm^{-1}]	24476±371	-2434±543	147±121	-189±158	504±172	0.8631	20
	24415±361	-2349±516	-	-	584±142	0.8476	20
v_{fluo} [cm^{-1}]	24334±1237	-3426±1809	-5092±404	269±526	-423±572	0.9663	20
	23688±943	-2409±1360	-5076±238	-	-	0.96040	20
Δv_{SS} [cm^{-1}]	141±1263	992±1848	5239±413	-457±538	927±584	0.9678	20
	761±160	-	5035±271	-	854±425	0.9656	20
Φ	0.54±0.37	0.22±0.54	-0.48±0.12	0.43±0.16	-0.37±0.17	0.7755	20
	0,70±0.05	-	-0.47±0.12	0.43±0.15	-0.41±0.13	0.7730	20
τ [ns]	3.05±1.15	-0.22±1.67	0.63±0.39	1.42±0.58	-3.42±0.67	0.7598	19
	2.089±0.66	-	0.62±0.37	1.42±0.56	-3.38±0.58	0.7595	19
k_f*10^8[s^{-1}]	2.04±0.72	0.37±1.06	-1.68±1.06	0.79±0.37	-0.48±0.42	0.8649	19
	2.32±0.10	-	-1.71±0.24	0.67±0.36	-	0.8436	19
$k_{nr}*10^8$[s^{-1}]	1.68±1.32	-0.72±1.92	1.24±0.45	-2.21±0.66	4.08±0.77	0.7858	19
	1.19±0.18	-	1.20±0.43	-2.21±0.64	4.22±0.67	0.7838	19
μ^2*10^5	1.19±0.30	-0.34±0.44	-0.69±0.10	0.36±0.15	-0.27±0.18	0.8624	19
[cm^3/s]	0.97±0.04	-	-0.71±0.10	0.36±0.15	-0.20±0.16	0.8565	19

Table 7 ESI Estimated from eqn (4) adjusted coefficients $(v_x)_0$, a_{π^*}, b_α, c_β their standard error and correlation coefficient (r^2) of the multiple linear correlation analysis of absorption (v_{abs}), fluorescence (v_{fluo}) wavenumber, Stokes shift (Δv_{SS}), fluorescence quantum yield (ϕ), fluorescence (k_f) and nonradiative (k_{nr}) rate constant and value proportional to squared transition dipole moment (μ^2)~$k_f/(n^2\ v_{fluo}{}^3$) of 1NacDMA as a function of Kamlet-Taft parameter solvent scale. N.p. denote number of solvent using in the analysis.

	$(v_x)_0$	a_{π^*}	b_α	c_β	r^2	N.p.
v_{abs} [cm^{-1}]	28962±147	-927±351	11677±142	-866±315	0.8664	20
v_{fluo} [cm^{-1}]	26662±400	-4105±961	959±389	-4455±862	0.8821	20
Δv_{SS} [cm^{-1}]	2341±346	3178±830	208±336	3589±745	0.8651	20
	2354±339	3385±747	-	3458±701	0.8618	20
Φ	0.93±0.04	-0.11±0.10	-0.48±0.04	-0.50±0.09	0.9380	20
	0.90±0.03	-	-0.50±0.04	-0.56±0.07	0.9331	20
τ [ns]	0.92±0.25	2,08±0.82	-2.31±0.72	0.38±0.97	0.7403	17
	0.93±0.24	2.35±0.45	-2.11±0.51	-	0.7372	17
k_f*10^8[s^{-1}]	7.57±0.40	-3.88±1.33	0.42±1.15	-4.05±1.56	0.8802	17
	7.59±0.39	-4,13±1.11	-	-3.66±1.11	0.8790	17
$k_{nr}*10^8$[s^{-1}]	0.67±1.47	-1.20±4.88	37.77±4.25	2.00±5.76	0.9244	17
	0.77±0.81	-	38.81±2.68	-	0.9237	17
μ^2*10^5	2.16±0.15	0.59±0.49	-0.40±0.43	-0.89±0.58	0.6195	17
[cm^3/s]	2.17±1.22	0.14±0.44	-3.72±1.47	-1.28±0.51	0.7825	15
	2.14±0.11	-	-3.84±1.38	-1.43.±0.26	0.7804	15

Table 8 ESI Estimated from eqn (4) adjusted coefficients $(v_x)_0$, a_{π^*}, b_α, c_β their standard error and correlation coefficient (r^2) of the multiple linear correlation analysis of absorption (v_{abs}), fluorescence (v_{fluo}) wavenumber, Stokes shift (Δv_{SS}), fluorescence quantum yield (ϕ), fluorescence (k_f) and nonradiative (k_{nr}) rate constant and value proportional to squared transition dipole moment (μ^2)~$k_f/(n^2\ v_{fluo}{}^3$) of 2NacDMA as a function of Kamlet-Taft parameter solvent scale. N.p. denote number of solvent using in the analysis.

	$(v_x)_0$	a_{π^*}	b_α	c_β	R^2	N
v_{abs} [cm^{-1}]	28190±148	1008±356	1183±144	-1217±319	0.8852	20
v_{fluo} [cm^{-1}]	27351±537	-5937±1288	455±521	-2721±1155	0.8052	20
	27380±523	-5486±1171	-	-3008±1099	0.7960	20
Δv_{SS} [cm^{-1}]	839±535	6945±1283	728±519	1450±1150	0.8282	20
Φ	0.850±0.050	0.098±0.102	-0.527±0.049	-0.485±0.108	0.9044	20
	0.873±0.041	-	-0.511±0.044	-0.430±0.084	0.9004	20
τ [ns]	0.75±0.27	2.15±0.89	-2.10±0.78	0.24±0.11	0.6932	17
k_f*10^8[s^{-1}]	8.08±0.70	-3.39±2.32	0.05±2.02	-3.39±2.74	0.6817	17
	8.08±0.67	-4.00±1.92	-	-3.34±1.93	0.6816	17
$k_{nr}*10^9$[s^{-1}]	1.34±2.38	-2.79±7.91	56.74±6.89	1.64±9.34	0.9104	17
	0.65±1.32	-	57.34±4.68	-	0.9092	17
μ^2*10^5	2.16±0.22	0.82±0.74	-0.06±0.65	-0.07±0.88	0.2570	17
[cm^3/s]	2.13±0.14	0.06±0.51	-4.30±1.67	1.04±0.58	0.6410	15
	2.14±0.12	-	-4.26±1.56	0.98±0.30	0.6405	15

Table 9 ESI Estimated from eqn (4) adjusted coefficients $(v_x)_0$, a_{π^*}, b_α, c_β their standard errors and correlation coefficient (r^2) of the multiple linear correlation analysis of absorption (v_{abs}), fluorescence (v_{fluo}) wavenumber, Stokes shift (Δv_{SS}), fluorescence quantum yield (ϕ), fluorescence (k_f) and nonradiative (k_{nr}) rate constant and value proportional to squared transition dipole moment (μ^2)~$k_f/(n^2\ v_{fluo}{}^3$) of AacDMA as a function of Kamlet-Taft parameter solvent scale. N.p. denote number of solvent using in the analysis.

	$(v_x)_0$	a_{π^*}	b_α	c_β	R^2	N
v_{abs} [cm^{-1}]	22882±66	-15±159	573±64	-279±143	0.8653	20
	22878±54	-	571±57	-288±109	0.8652	20
v_{fluo} [cm^{-1}]	22212±492	-4500±1180	568±477	-2489±1057	0.7608	20
Δv_{SS} [cm^{-1}]	669±514	4485±1234	6±499	2210±1106	0.7354	20
	669±498	4491±1096	-	2206±1029	0.7354	20
Φ	0.72±0.07	-0.29±0.18	-0.21±0.07	0.05±0.16	0.5120	20
	0.72±0.07	-0.25±0.14	-0.21±0.07	-	0.5089	20
τ [ns]	3.00±0.25	1.14±0.64	-0.63±0.26	0.31±0.60	0.4400	19
	3.02±0.24	1.36±0.46	-0.64±0.26	-	0.4299	19
k_f*10^8[s^{-1}]	2.35±1.58	-1.10±0.40	-0.30±0.17	-0.37±0.37	0.6688	19
	2.33±1.58	-1.37±0.30	-0.29±0.17	-	0.6470	19
$k_{nr}*10^8$[s^{-1}]	1.03±0.32	-0.04±0.82	0.93±0.34	0.32±0.72	0.3634	19
	1.12±0.18	-	0.95±0.31	-	0.3522	19
μ^2*10^5	1.00±0.06	-0.52±0.16	0.11±0.07	-0.11±0.15	0.6945	19
[cm^3/s]	1.00±0.06	-0.60±0.12	-0.10±0.06	-	0.6838	19

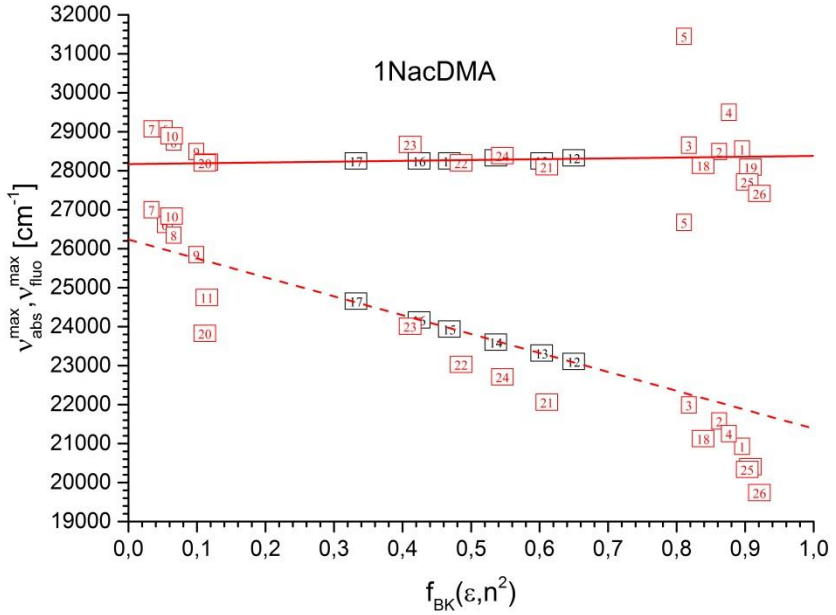

Fig. 27 ESI Plot of the correlation of ν_{abs}^{max} and ν_{fluo}^{max} *versus* Bilot-Kawski solvent polarity function $f_{BK}(\varepsilon,n^2)$ for 1NacDMA. Solid line represents the best fit for absorption, dashed line for emission. The black points denote 1-chloro-hydrocarbon solvents, red points other studied solvents. Numbers in the squares correspond to the order of the solvents in Tables 1-3 in the main text of publication.

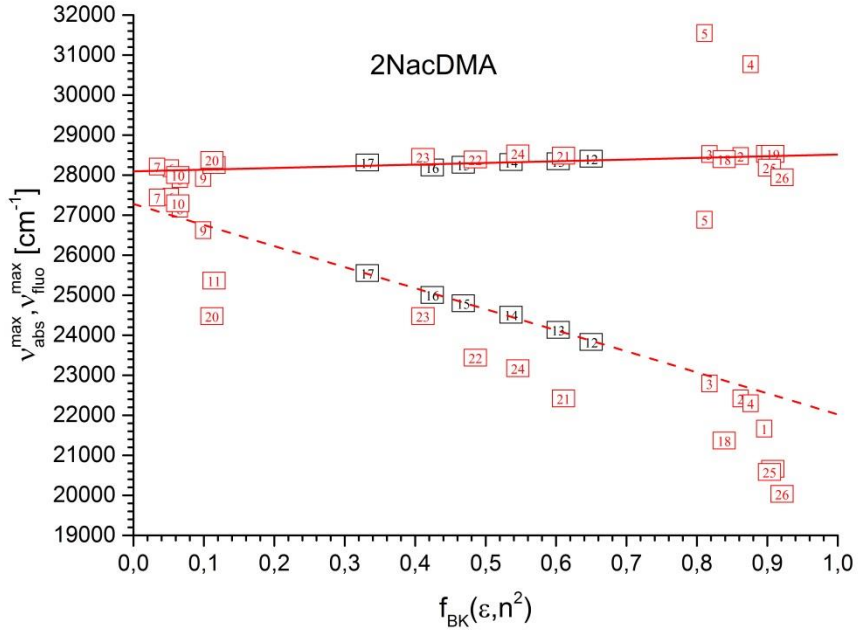

Fig. 28 ESI Plot of the correlation of ν_{abs}^{max} and ν_{fluo}^{max} *versus* Bilot-Kawski solvent polarity function $f_{BK}(\varepsilon,n^2)$ for 2NacDMA. Solid line represents the best fit for absorption, dashed line for emission. The black points denote 1-chloro-hydrocarbon solvents, red points other studied solvents. Numbers in the squares correspond to the order of the solvents in Tables 1-3 in the main text of publication.

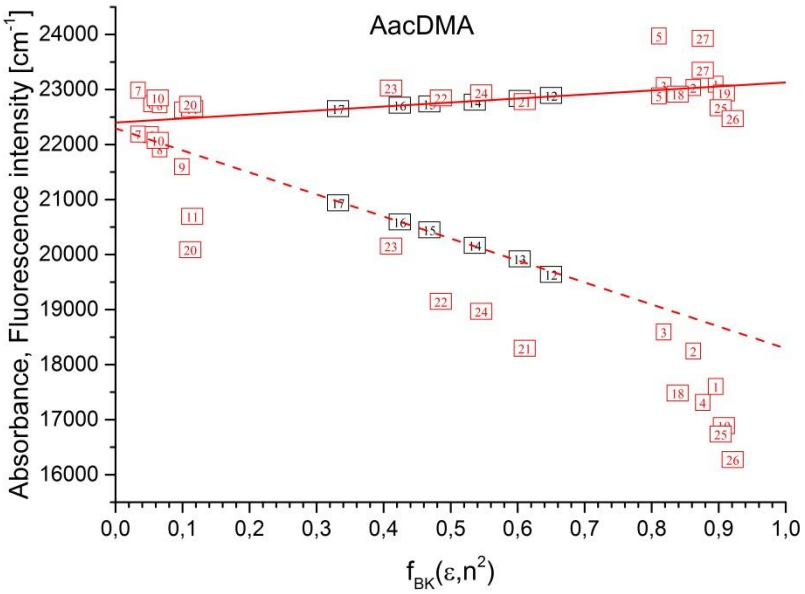

Fig. 29 ESI Plot of the correlation of ν_{abs}^{max} and ν_{fluo}^{max} *versus* Bilot-Kawski solvent polarity function $f_{BK}(\varepsilon,n^2)$ for AacDMA. Solid line represents the best fit for absorption, dashed line for emission. The black points denote 1-chloro-hydrocarbon solvents, red points other studied solvents. Numbers in the squares correspond to the order of the solvents in Tables 1-3 in the main text of publication.

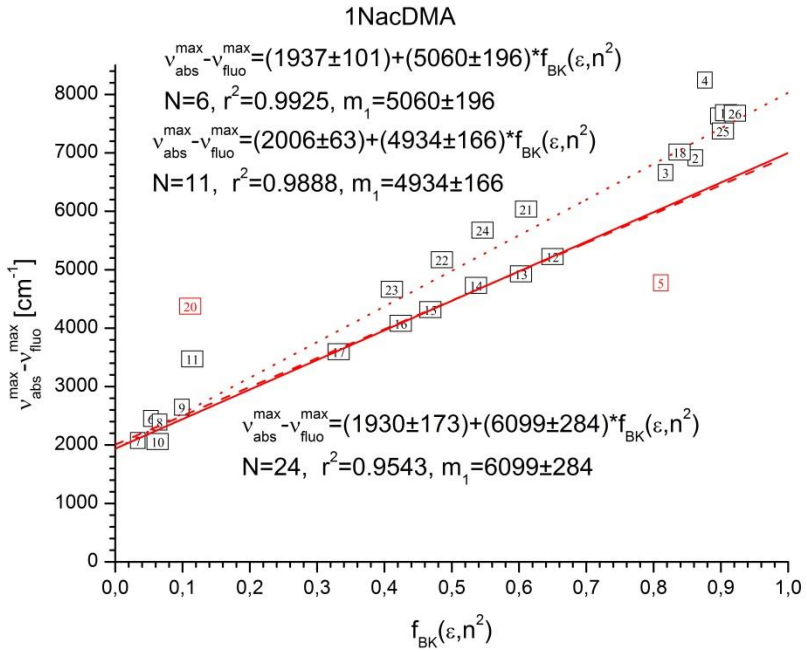

Fig. 30 ESI Plot of the correlation of ν_{abs}^{max}-ν_{fluo}^{max} *versus* Bilot-Kawski solvent polarity function $f_{BK}(\varepsilon,n^2)$ for 1NacDMA. Solid line represents the best fit for 1-chloro-hydrocarbon solvents, dashed line for 1-chloro-hydrocarbons and saturated hydrocarbon solvents, and dotted line for all solvents studied except 1,4-dioxane (20) and HFiP (5). Numbers in the squares correspond to the order of the solvents in Tables 1-3 in the main text of publication.

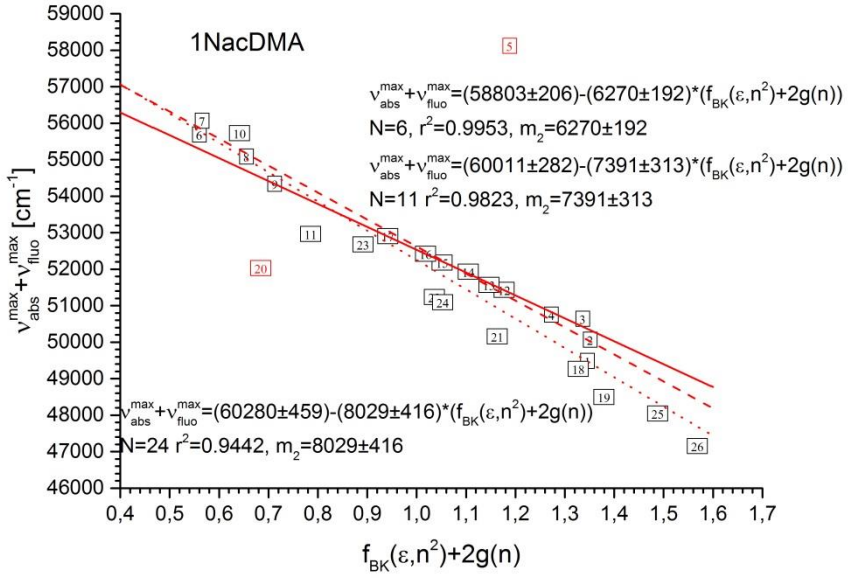

Fig. 31 ESI Plot of the correlation of ν_{abs}^{max}+ν_{fluo}^{max} *versus* Bilot-Kawski solvent polarity function $f_{BK}(\varepsilon,n^2)$+2g(n) for 1NacDMA. Solid line represents the best fit for 1-chloro-hydrocarbon solvents, dashed line for 1-chloro-hydrocarbons and saturated hydrocarbon solvents, and dotted line for all solvents studied except 1,4-dioxane (20) and HFiP (5). Numbers in the squares correspond to the order of the solvents in Tables 1-3 in the main text of publication.

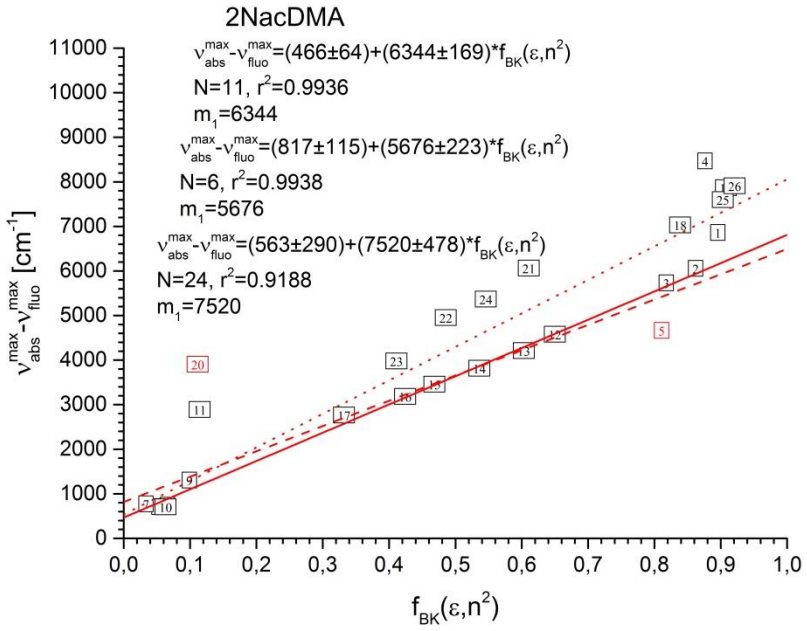

Fig. 32 ESI Plot of the correlation of ν^{max}_{abs}-ν^{max}_{fluo} *versus* Bilot-Kawski solvent polarity function $f_{BK}(\varepsilon,n^2)$ for 2NacDMA. Solid line represents the best fit for 1-chloro-hydrocarbon solvents, dashed line for 1-chloro-hydrocarbons and saturated hydrocarbon solvents, and dotted line for all solvents studied except 1,4-dioxane (20) and HFiP (5). Numbers in the squares correspond to the order of the solvents in Tables 1-3 in the main text of publication.

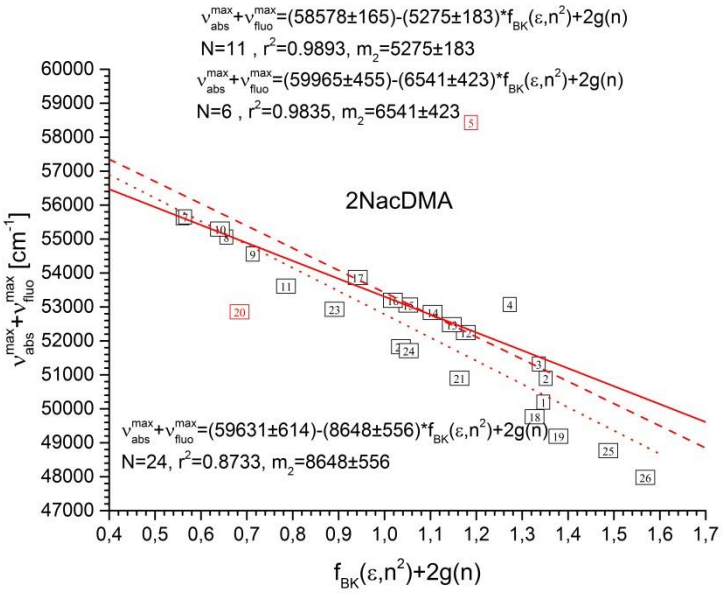

Fig. 33 ESI Plot of the correlation of ν^{max}_{abs}+ν^{max}_{fluo} *versus* Bilot-Kawski solvent polarity function $f_{BK}(\varepsilon,n^2)$+2g(n) for 2NacDMA. Solid line represents the best fit for 1-chloro-hydrocarbon solvents, dashed line for 1-chloro-hydrocarbons and saturated hydrocarbon solvents, and dotted line for all solvents studied except 1,4-dioxane (20) and HFiP (5). Numbers in the squares correspond to the order of the solvents in Tables 1-3 in the main text of publication.

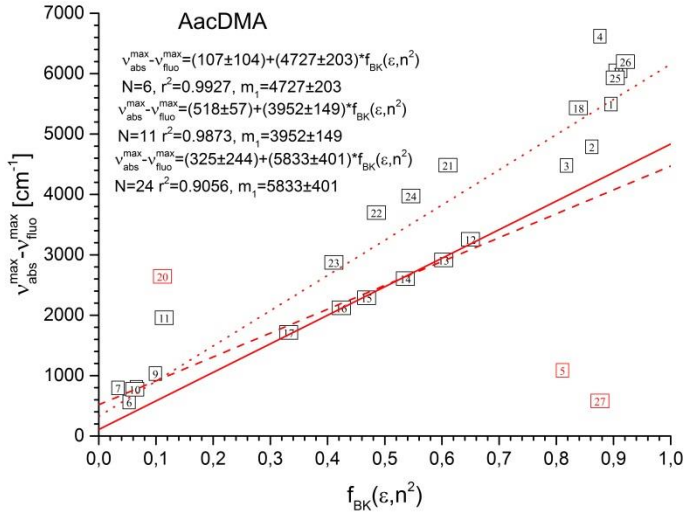

Fig. 34 ESI Plot of the correlation of ν_{abs}^{max} -ν_{fluo}^{max} *versus* Bilot-Kawski solvent polarity function $f_{BK}(\varepsilon,n^2)$ for AacDMA. Solid line represents the best fit for 1-chloro-hydrocarbon solvents, dashed line for 1-chloro-hydrocarbons and saturated hydrocarbon solvents, and dotted line for all solvents studied except 1,4-dioxane (20) and HFiP (5). Numbers in the squares correspond to the order of the solvents in Tables 1-3 in the main text of publication.

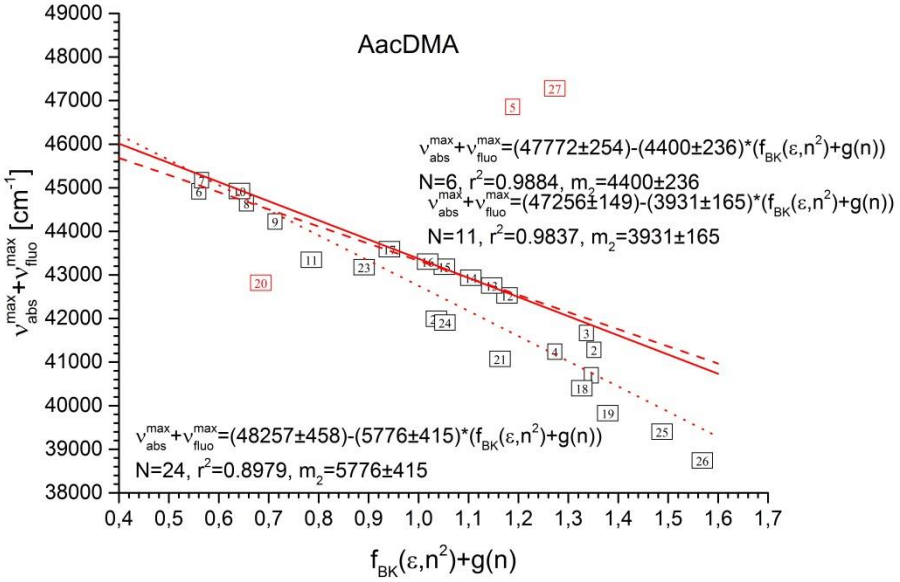

Fig. 35 ESI Plot of the correlation of $\nu_{abs}^{max}+\nu_{fluo}^{max}$ *versus* Bilot-Kawski solvent polarity function $f_{BK}(\varepsilon,n^2)+2g(n)$ for AacDMA. Solid line represents the best fit for 1-chloro-hydrocarbon solvents, dashed line for 1-chloro-hydrocarbons and saturated hydrocarbon solvents, and dotted line for all solvents studied except 1,4-dioxane (20) and HFiP (5) and short wavelength band in TFE(27). Numbers in the squares correspond to the order of the solvents in Tables 1-3 in the main text of publication.

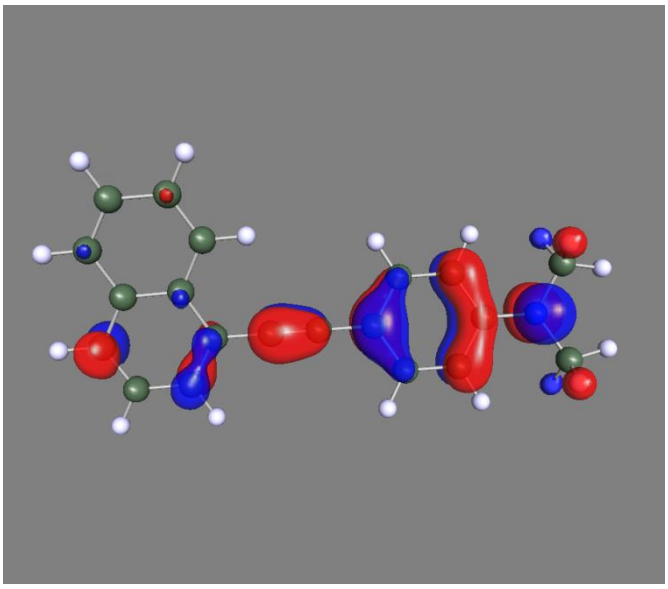

Fig. 36 ESI HOMO orbital of 1NacDMA

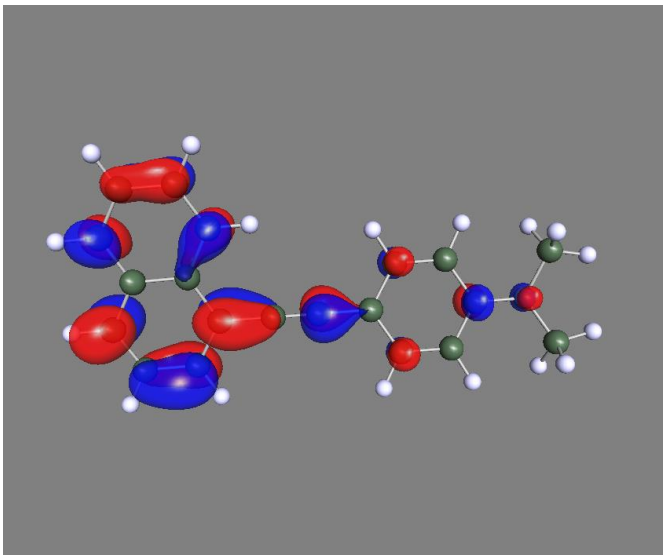

Fig. 37 ESI LUMO orbital of 1NacDMA

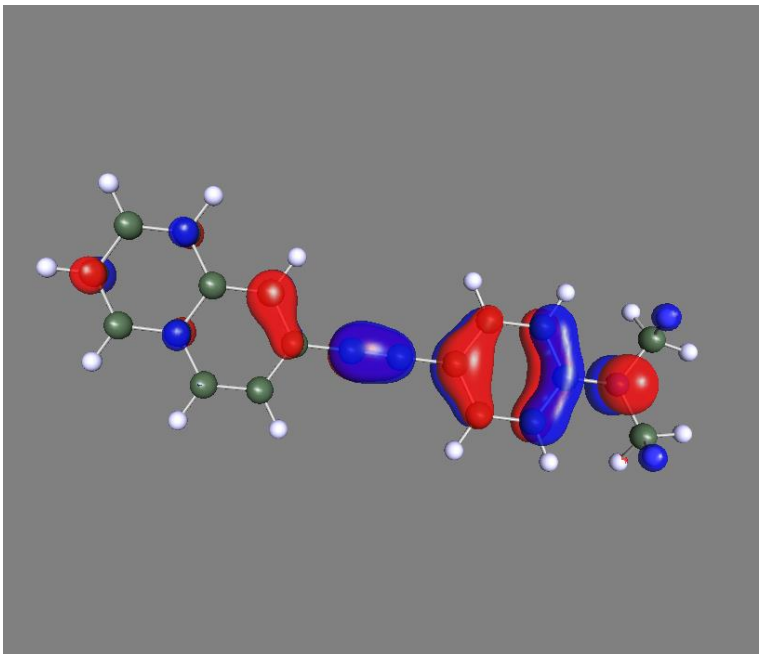

Fig. 38 ESI HOMO orbital of 2NacDMA

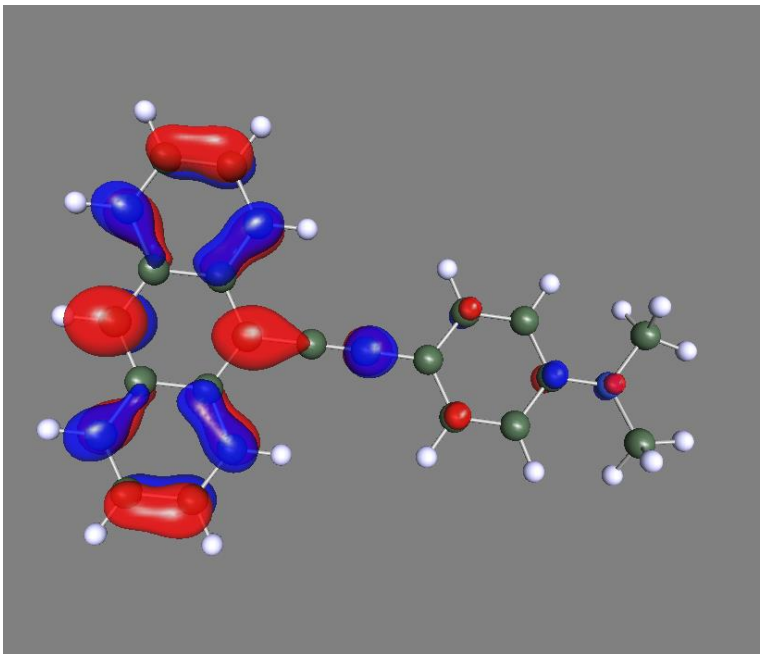

Fig. 39 ESI LUMO orbital of 2NacDMA

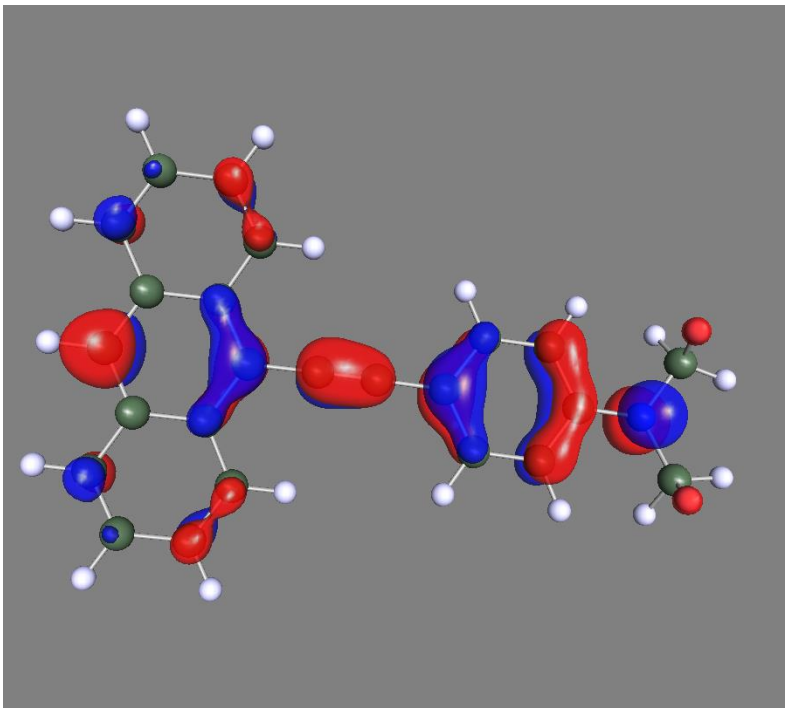

Fig. 40 ESI HOMO orbital of AacDMA

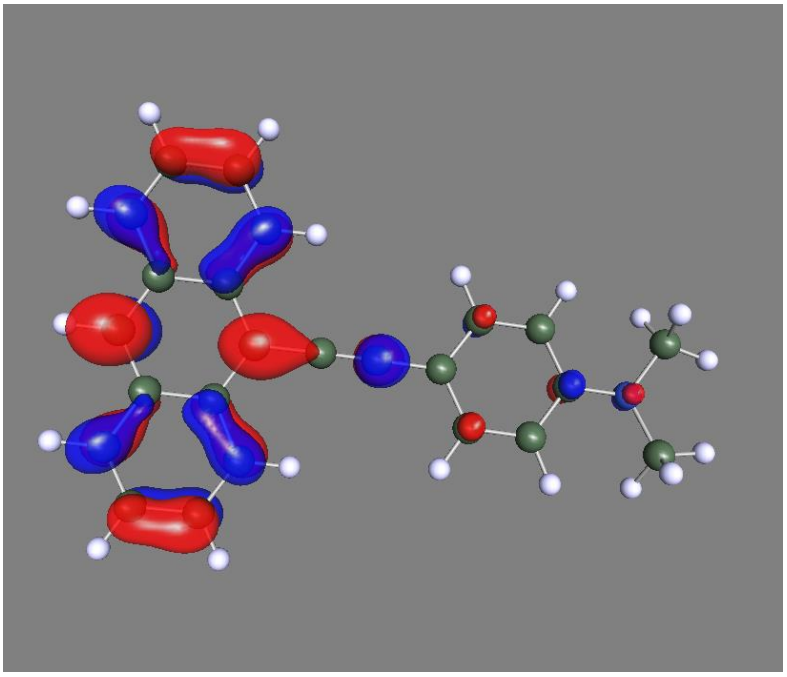

Fig. 41 ESI LUMO orbital od AacDMA

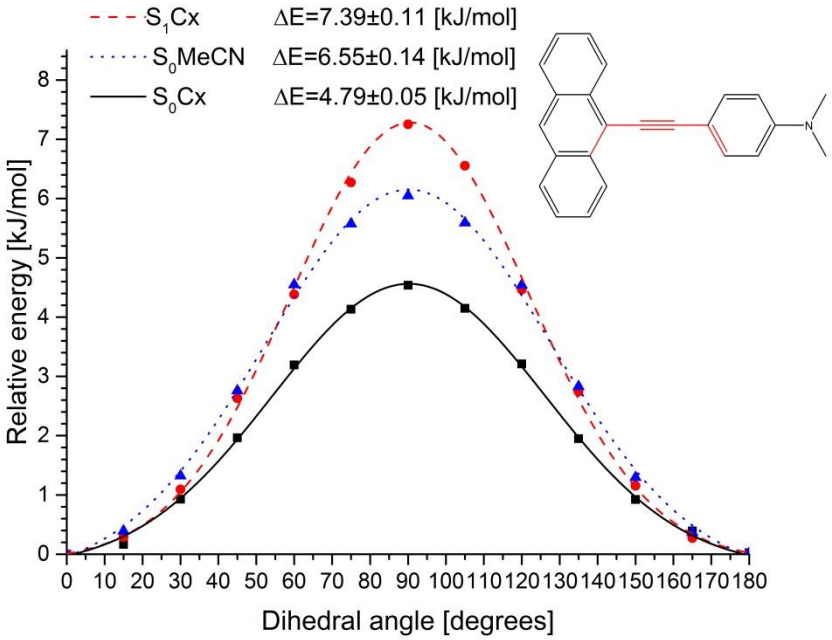

Fig. 42 ESI The dependence of energy on dihedral angle for AacDMA. Lines denote the best fit of Gaussian function to the calculated points. Solid black line for ε=2 (cyclohexane in the ground state), blue dotted line for ε=37.5 (acetonitrile in the ground state),dashed red line ε=2 (cyclohexane in the excited state).

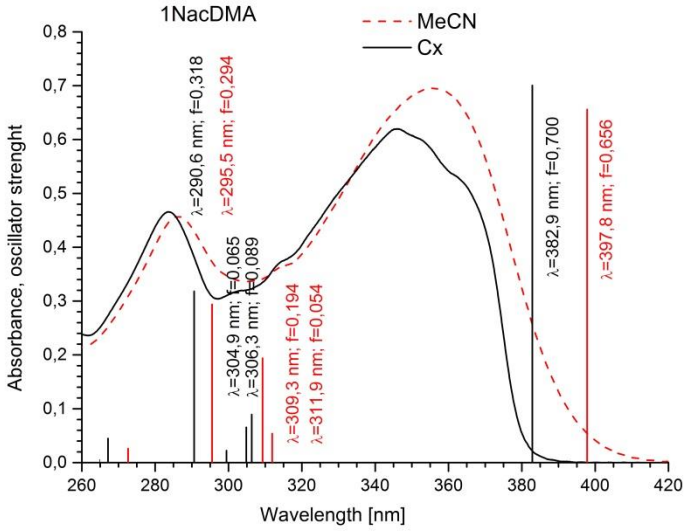

Fig. 43 ESI Absorption spectra of 1NacDMA in cyclohexane (black line) and acetonitrile (red line) and calculated vertical transitions in absorption for ε=2 (cyclohexane, black vertical lines) and ε=37.5 (acetonitrile, red vertical lines).

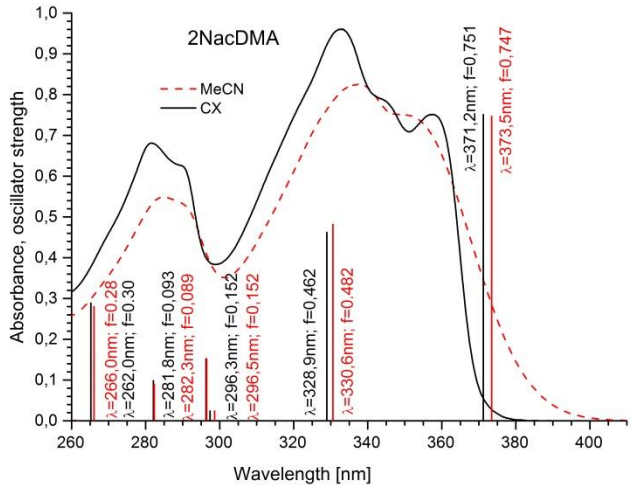

Fig. 44 ESI Absorption spectra of 2NacDMA in cyclohexane (black line) and acetonitrile (red line) and calculated vertical transitions in absorption for ε=2 (cyclohexane, black vertical lines) and ε=37.5 (acetonitrile, red vertical lines).

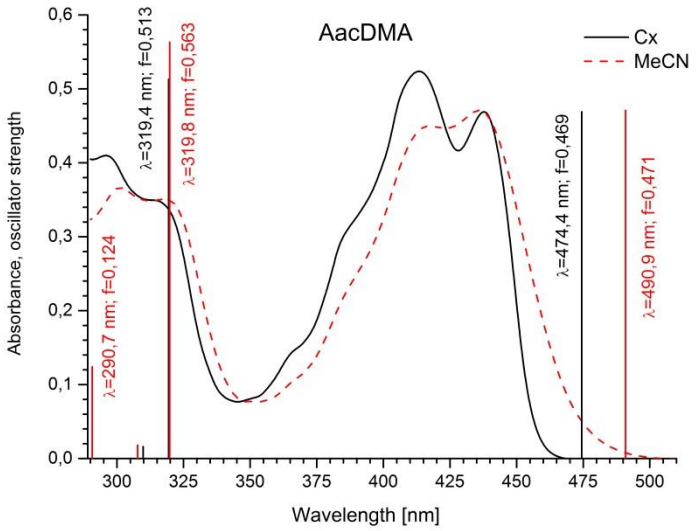

Fig. 45 ESI Absorption spectra of AacDMA in cyclohexane (black line) and acetonitrile (red line) and calculated vertical transitions in absorption for ε=2 (cyclohexane, black vertical lines) and ε=37.5 (acetonitrile, red vertical lines).

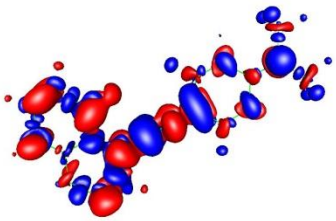

Fig. 46 ESI The difference of electron density between the excited and ground state for 1NacDMA. The blue color denotes decrease and red increase of electron density.

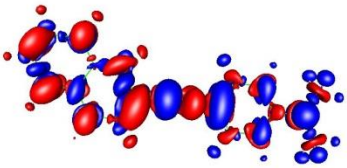

Fig. 47 ESI The difference of electron density between the excited and ground state for 2NacDMA. The blue color denotes decrease and red increase of electron density.

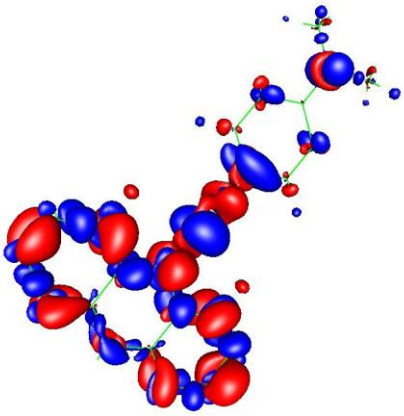

Fig. 48 ESI The difference of electron density between the excited and ground state for AacDMA. The blue color denotes decrease and red increase of electron density.

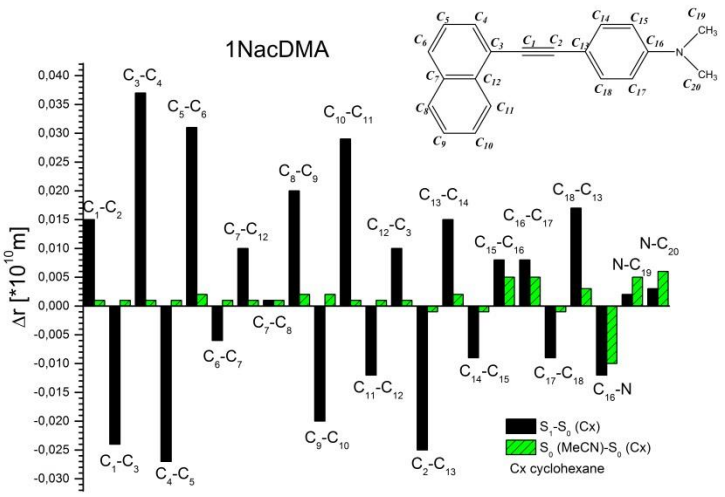

Fig. 49 ESI The changes in the bond lengths between the optimized structures calculated in excited and ground state for ε=2 (black bars) as well as between optimized structures calculated in the ground state for ε=37.5 and ε=2 for 1NacDMA.

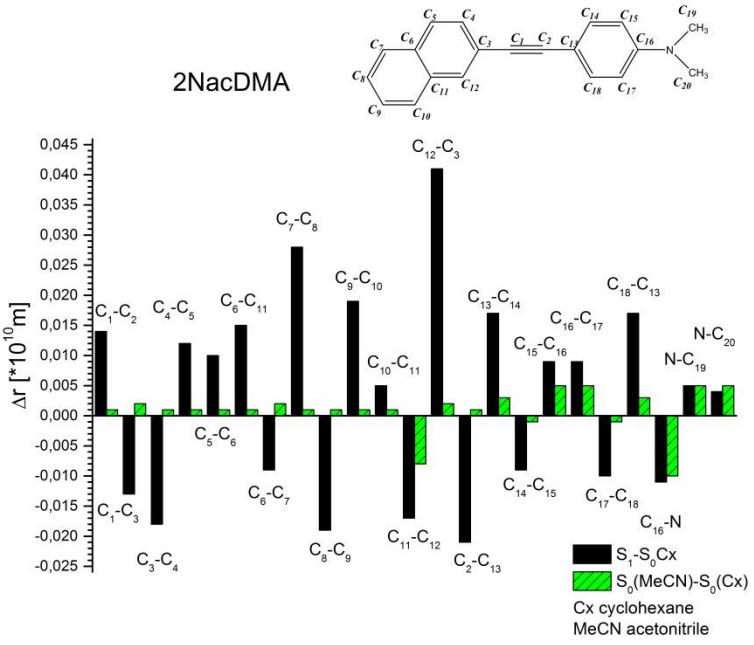

Fig. 50 ESI The changes in the bond lengths between the optimized structures calculated in excited and ground state for ε=2 (black bars) as well as between optimized structures calculated in the ground state for ε=37.5 and ε=2 for 2NacDMA.

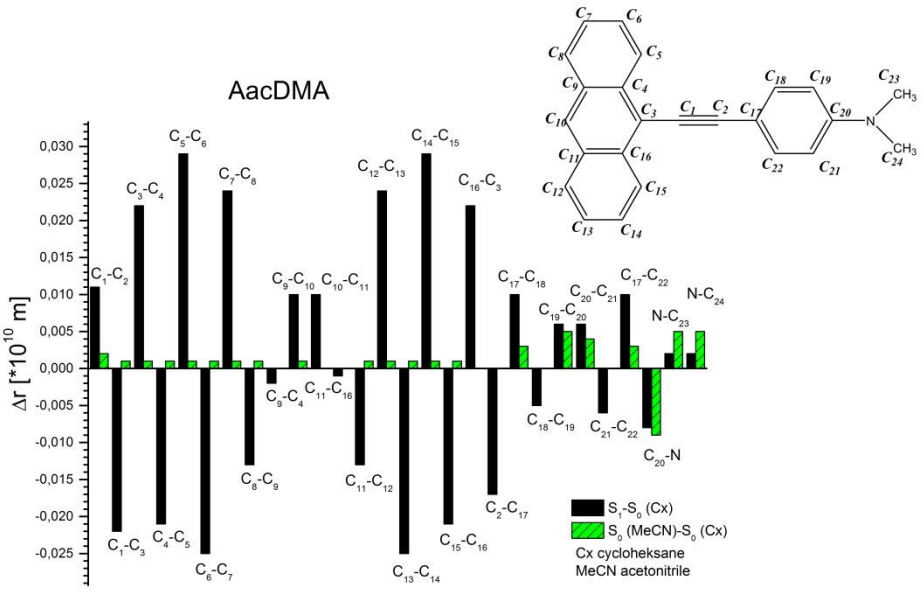

Fig. 51 ESI The changes in the bond lengths between the optimized structures calculated in excited and ground state for ε=2 (black bars) as well as between optimized structures calculated in the ground state for ε=37.5 and ε=2 for AacDMA.